

**Features in the NMR spectra of the aglycones of *Agave* spp. saponins. HMBC method for aglycone identification (HMAI)**

Journal:	<i>Phytochemical Analysis</i>
Manuscript ID	PCA-20-0082
Wiley - Manuscript type:	Special Issue Review
Date Submitted by the Author:	20-Feb-2020
Complete List of Authors:	Simonet, Ana M; Universidad de Cádiz, Química Orgánica Duran, Alexandra G.; University of Cadiz Faculty of Sciences, Organic chemistry Perez, Andy; Universidad de Concepción, Análisis Instrumental Macías, Francisco A.; Univeristy of Cadiz, Organic Chemistry
Keywords:	Agave, HMBC, HMAI, 1H and 13C NMR, saponin aglycone identification

SCHOLARONE™  
Manuscripts

1 **Features in the NMR spectra of the aglycones of *Agave spp.* saponins.**

2 **HMBC method for aglycone identification (HMAI)**

3 **Short title:** HMBC Method for aglycone identification (HMAI) of *Agave spp.* saponins

4

5 Ana M. Simonet<sup>1</sup>, Alexandra G. Durán<sup>1</sup>, Andy J. Pérez<sup>2</sup>, and Francisco A. Macías<sup>1</sup>

6

7

8 <sup>1</sup> Allelopathy Group, Department of Organic Chemistry, Institute of Biomolecules  
9 (INBIO), Campus de Excelencia Internacional (ceiA3), School of Science, University of  
10 Cadiz, C/ República Saharaui nº 7, 11510 Puerto Real, Cadiz, Spain.

11 <sup>2</sup> Departamento de Análisis Instrumental, Facultad de Farmacia, Universidad de  
12 Concepción, Concepción 4191996, Chile.

13

14 **Correspondence**

15 Ana M. Simonet and Francisco A. Macías, Department of Organic Chemistry, School of  
16 Science, University of Cadiz, C/ República Saharaui nº 7, 11510 Puerto Real, Cadiz,  
17 Spain. Phone: +34 956012770; fax: +34 956016193; e-mail: [ana.simonet@uca.es](mailto:ana.simonet@uca.es);  
18 [famacias@uca.es](mailto:famacias@uca.es)

19

20 **Funding information**

21 Ministerio de Economía, Industria y Competitividad (MINEICO) of Spain, Grant  
22 number: AGL2017-88083-R.

23

25 **Abstract**

26

27 **Introduction:**

28 The analysis and detection of steroidal saponins is mainly performed using  
29 chromatographic techniques coupled with Mass Spectrometry. However, Nuclear  
30 Magnetic Resonance (NMR) spectroscopy is a potential tool that can be combined with  
31 these techniques to obtain an unambiguous structural characterization.

32 **Objective:**

33 This work provides a review of the  $^{13}\text{C}$  and  $^1\text{H}$  NMR spectroscopic data of aglycones  
34 from *Agave* saponins reported in the literature and also the development of an easy  
35 identification method for these natural products.

36 **Methods:**

37 The database Scifinder was used for spectroscopic data collection in addition to data  
38 obtained from the Cadiz Allelopathy research group. The keywords used were *Agave*,  
39 spirostanic, furostanic, and saponin.

40 **Results:**

41 The shielding variations produced by functional groups on the aglycone core and the  
42 structural features of the most representative aglycones from *Agave* species are  
43 described. The effects are additive for up to four long-range connectivities. A method  
44 for the identification of aglycones (HMAI) is proposed to classify aglycones from  
45 *Agave* spp. through the use of  $^1\text{H}$  NMR and HMBC experiments.

46 **Conclusions:**

47 The HMBC spectrum is representative of the structural features of aglycones from  
48 *Agave* spp. The HMAI method allowed the identification of pure saponins or mixtures  
49 thereof and this method can be used in combination with chromatographic techniques

50 coupled with Mass Spectrometry to provide a more thorough analysis of *Agave* samples  
51 that contain aglycones.

52 **Short abstract**

53  $^1\text{H}$  and  $^{13}\text{C}$  shielding variations produced by functional groups on the aglycone core and  
54 the structural features of the most representative aglycones from *Agave* species are  
55 described. The effects are additive for up to four long-range connectivities. A method  
56 for the identification of aglycones (HMAI) is proposed to classify aglycones from  
57 *Agave* spp. through the use of  $^1\text{H}$  NMR and HMBC experiments. This method allowed  
58 the identification of pure saponins or mixtures thereof and it could be used in  
59 combination with chromatographic techniques coupled with Mass Spectrometry to  
60 provide a more thorough analysis of *Agave* samples that contain aglycones.

61

62 **Keywords:** saponin, aglycone, *Agave*, HMBC, HMAI,  $^1\text{H}$  NMR,  $^{13}\text{C}$  NMR,  
63 identification

65

66 **1. INTRODUCTION**67 **1.1. Saponins. Definition and biological activities**

68 Saponins are secondary metabolites that are glycosidic in character and have specific  
69 natural properties. Despite their well-known biological activities, the specific role and  
70 mechanism of action of saponins are not fully established. It has been suggested that  
71 saponins could play a significant defensive role against microorganisms, because  
72 various fungi produce saponin-detoxifying enzymes,<sup>1</sup> and against mammals or insect  
73 herbivores as an antifeedant.<sup>2</sup> Moreover, physiological effects associated with plant  
74 growth regulation and development have been reported as possible functions for  
75 saponins.<sup>3</sup>

76 These natural products, which are found in a vast variety of plant species and in some  
77 marine organisms, consist of a hydrophobic triterpene or sterol backbone and a  
78 hydrophilic carbohydrate chain formed by monosaccharide units, with the structural  
79 features linked together by a glycosidic bond (Figure 1). Based on the structures of the  
80 aglycone skeletons, saponins can be divided into two main groups, namely steroidal and  
81 triterpenoid saponins. Triterpenoid saponins are mostly found in dicotyledonous species  
82 whereas monocots mainly produce steroidal saponins.<sup>2,4</sup> Steroidal saponins have a  
83 hydrophobic nucleus or sapogenin constituted by 27 carbon atoms.

84 The amphipathic nature of saponins means that they can act as surfactants and in most  
85 cases stable they give soap-like foams in aqueous solutions and they have been used as  
86 natural soaps and detergents since ancient times.<sup>5</sup> The aforementioned properties  
87 allowed these compounds to rupture erythrocytes and cause irreversible damage to the  
88 membrane lipid bilayer. This hemolytic activity is one of the first effects reported and is

89 mode of action that is most widely accepted for the biological activities shown by  
90 saponins.<sup>6</sup> However, in a study performed by Wang and co-workers the correlation  
91 between hemolytic and cytotoxic activities of a collection of steroidal saponins was  
92 evaluated. The results indicated that cytotoxic activity does not always relate with  
93 hemolytic activity, thus suggesting that steroidal saponins execute the two activities in  
94 different mechanisms.<sup>7</sup>

95 It has been demonstrated that the biological activities of saponins are dependent on their  
96 structures. For example, a thorough study of 28 sapogenins and spirostane-type  
97 saponins against pathogenic fungi showed that those saponins with less oxygenation in  
98 the steroidal core and a sugar moiety of four or five monosaccharide units exhibited  
99 significant activity.<sup>8</sup> The phytotoxicity of these secondary metabolites has also been  
100 tested. The effects of 28 steroidal saponins on the standard target species *Lactuca sativa*  
101 were evaluated. Strong root growth inhibition was noted for those saponins with four or  
102 more sugar units in the saccharide chain and oxygenation, especially at the C-12  
103 position of the aglycone skeleton.<sup>9-11</sup> Moreover, in other studies it has been  
104 demonstrated that the activity is highly dependent on the monosaccharide features.<sup>12</sup>  
105 Likewise, other structure-activity relationship studies (SARs) of steroidal saponins on  
106 HL-60 (human promyelocytic leukemia) cells showed that cytotoxicity was dependent  
107 on the aglycone backbone and also the sugar moieties and their sequences.<sup>13</sup> These  
108 results indicated that the cytotoxic effects shown by these saponins could be due to non-  
109 specific detergent effects with changes in membrane architecture. Nonetheless, the level  
110 of damage is considerably different among the saponins tested, and two of them with  
111 two sugar residues in the carbohydrate chain caused cell death through an apoptotic  
112 process. Other saponins with these structural features have shown other mechanisms of  
113 action.<sup>14,15</sup>

114 All of the findings outlined above support the idea that mechanisms other than  
115 membrane damage are also involved.

116 The genus *Agave* is one of the main sources of steroidal saponins. The sugar moieties  
117 present in saponins from this genus are  $\beta$ -D-glucopyranosyl,  $\beta$ -D-galactopyranosyl,  $\beta$ -  
118 D-xylopyranosyl and  $\alpha$ -L-rhamnopyranosyl units.<sup>16</sup> On the one hand, taking into  
119 account the sapogenin backbone, saponins of *Agave* can be classified as spirostanol  
120 glycosides and furostanol glycosides. On the other hand, monodesmosidic saponins are  
121 those in which the sugar chain is present at only one position (generally at C-3) of the  
122 sapogenin, while bidesmosidic saponins have two sugar units located at two different  
123 points of the aglycone core. Most of the bidesmosidic furostanol saponins are  
124 glycosylated at the C-3 and C-26 positions, with a  $\beta$ -D-glucopyranoside usually present  
125 in the latter position.

## 126 **1.2. Drawbacks in the isolation and elucidation of saponins. Analysis of** 127 **mixtures.**

128 There are several methods to obtain saponin-rich extracts, including conventional  
129 (maceration, Soxhlet and reflux extraction) and green (ultrasound-assisted, microwave-  
130 assisted and accelerated solvent extraction) techniques.<sup>17</sup> Crude extracts are commonly  
131 mixtures of saponins with a wide range of polarities and structural diversity, differing  
132 even between plant organs. Steroidal saponins with up to seven sugar units have been  
133 reported.<sup>18</sup> Thus, the isolation of saponins remains a challenge and requires the use of  
134 various separation techniques and different adsorbents to achieve, in most cases, the  
135 isolation of the major saponins.

136 *Agaves* have been widely used for their high carbohydrate content to obtain *Agave* sap,  
137 sweeteners and, after fermentation, alcoholic beverages such as pulque, mescal or

138 tequila. Chromatographic techniques coupled with mass spectrometry have been used to  
139 determine the saponins content and biochemical changes that occur during beverage  
140 processing. Thus, for instance, this methodology has allowed the quantification and  
141 identification of saponins in wild and cultivated populations used for the production of  
142 mescal and pulque,<sup>19</sup> after the use of micropropagation to allow mass production of  
143 *Agaves*,<sup>20</sup> under *in vitro* drought stress,<sup>21</sup> their variation during plant ripening stage,<sup>22,23</sup>  
144 in concentrated *Agave* sap produced in different states of Mexico,<sup>24</sup> or changes in the  
145 saponins profile by microorganisms after *Agave* sap fermentation.<sup>25</sup>

146 Mass spectrometry is a valuable tool that provides structural information on saponins,  
147 including the fragmentation pattern of the sugar chain. This technique allows the  
148 assignment and quantification of the saponins previously isolated from the species being  
149 analyzed. However, structural assignment of saponins from different species cannot be  
150 achieved, since there are isomers with identical masses and fragmentation patterns.

151 Given the influence of the structure on the biological activity of saponins, it would be  
152 beneficial to complete these studies with nuclear magnetic resonance (NMR)  
153 spectroscopic techniques. These experiments provide unambiguous information on the  
154 position and stereochemistry of the functional groups present in the aglycone, as well as  
155 the nature and connectivity of the different sugars on the carbohydrate chain.

### 156 **1.3. Evolution of the structural elucidation and assignment procedures**

157 The first studies that addressed the structural elucidation of secondary metabolites from  
158 the *Agave* genus were focused on sapogenins.<sup>26</sup> Physical properties such as melting  
159 point determination and chemical transformations, including elemental analysis and  
160 oxidation and reduction (redox) reactions, were the most common techniques used for  
161 the determination of known compounds. For a few years, the detection of certain



162 sapogenins was performed by measuring the ultraviolet absorption maximum<sup>27</sup> in the  
163 typical region for an  $\alpha,\beta$ -unsaturated ketone system. This approach allowed the  
164 identification of 9-dehydrospirostan-12-ones.

165 The first structural elucidation of saponins was carried out by the total hydrolysis of the  
166 isolated saponins followed by determination of melting point, IR, MS and  
167 chromatographic mobility to identify the corresponding aglycone.<sup>28</sup> Specific techniques  
168 were subsequently applied to identify the monosaccharides. Interglycosidic linkages  
169 were determined by acid hydrolysis and permethylation followed by acid hydrolysis of  
170 these units to obtain the different protosaponins. The identification of monosaccharides  
171 was achieved by comparison with known samples. In some cases, these methods were  
172 combined with mass spectrometry or FAB-MS to ascertain the sequence of sugars.<sup>29</sup>

173 The presence of furostane-type saponins was determined by thin layer chromatography  
174 using Ehrlich's reagent for a preliminary examination and subsequent conversion to  
175 their spirostanic derivatives through specific enzymes facilitated their further  
176 elucidation.<sup>30</sup>

177 In the early years, NMR techniques were used for the identification of the aglycone  
178 moiety after a hydrolysis reaction.<sup>31</sup> <sup>13</sup>C NMR experiments proved to be very useful for  
179 the determination of less complex saponins. Thus, glycosylation shift rules began to be  
180 applied to determine characteristic signal shifts (downfield or upfield) at the  $\alpha$ - and  $\beta$ -  
181 positions with respect to the -OH groups that were glycosylated.<sup>32,33</sup> Sugar chains with  
182 up to six units were elucidated using the fragmentation patterns observed by mass  
183 spectrometry and by comparison with <sup>13</sup>C NMR data reported in the literature.<sup>34</sup>

184 The characterization of these secondary metabolites is not an easy task but the advances  
185 in NMR technology have provided a non-destructive way to achieve this

186 characterization. The emergence of two-dimensional NMR experiments allowed the  
187 elucidation and signal assignment to be carried out in a more thorough and reliable  
188 way.<sup>35</sup> One of the main advantages is that an unambiguous characterization of complex  
189 sugar moieties can be achieved. Sugar linkage analysis and spatial arrangements can be  
190 determined by HMBC and 1D or 2D NOESY/ROESY experiments.<sup>36</sup>

191 These two-dimensional NMR experiments have been used since around 2000 for the  
192 determination of saponins and this technique requires a lower amount of pure  
193 compound. Moreover, the development of higher field NMR spectrometers (at least 500  
194 MHz) has made the complete assignments of the <sup>1</sup>H NMR spectra feasible, especially in  
195 overlapping zones.<sup>37</sup>

196 As mentioned previously, these metabolites have potentially attractive biological  
197 activities. Given that there is a high structure-activity correlation, including the  
198 oxygenation pattern of the aglycone and nature of the sugar moiety, it is crucial to  
199 achieve the most unambiguous determination possible.

200 Furthermore, because of the amphipathic nature of these compounds and the presence of  
201 structurally related forms with very similar polarities, their separation can be tricky and  
202 LC-MS and NMR techniques have been used to screen saponins by hyphenated  
203 analytical platforms<sup>38</sup> or metabolomics.<sup>39</sup>

## 204 **2. SALIENT AND COMMON FEATURES IN THE NMR SPECTRA OF** 205 **SAPONIN AGLYCONES FROM *AGAVE* SPP.**

206 A systematic compilation of the <sup>13</sup>C NMR chemical shifts for steroidal-type saponins  
207 dates from the 1980s.<sup>40</sup> Reviews covering the most characteristic <sup>13</sup>C signals to  
208 determine the ring fusion and spirostane/furostane skeleton have been published.<sup>35</sup>

209 Likewise, taking into account the  $^1\text{H}$  NMR chemical shift patterns of methylene C-26 of  
210 a range of saponins, the stereochemistry of C-25 could be ascertained.<sup>41–43</sup>

211 Recently, a comprehensive review of the structural features of saponins from *Agave*  
212 species was published by Sidana and co-workers.<sup>16</sup> The present review will focus on the  
213 influence of the main structural characteristics of  $^1\text{H}$  and  $^{13}\text{C}$  chemical shifts and will  
214 also provide an exhaustive overview of patterns and signals that could be key clues to  
215 identify the aglycone. The significant signals due to either their sensitivity to  
216 neighboring functional groups or their fast and feasible detection in one- and two-  
217 dimensional spectra will also be discussed.

218 It is unusual to find the full assignments of the  $^1\text{H}$  NMR data for steroidal saponins.  
219 Nonetheless, the chemical shifts of saponins with the main aglycone structural  
220 characteristics and the most common sugar chains have been selected (Tables 1 and 2).  
221 All NMR data were obtained from samples in deuterated pyridine in order to avoid the  
222 influence of the solvent on the chemical shift. This solvent is the most widely used for  
223 this kind of compound and it is able to dissolve saponins with a variable range of  
224 solubilities.<sup>35</sup>

225  $^1\text{H}$  and  $^{13}\text{C}$  spectroscopic data were adjusted by comparing the chemical shifts described  
226 at positions 22 and 27 using TMS as internal reference. Thus, for  $^1\text{H}$  NMR values, the  
227 setting is from 0 to  $-0.4$  ppm and for  $^{13}\text{C}$  NMR data from 0.4 to  $-0.3$  ppm (see  
228 supporting information).

229 The selected data show the consistency in the assignments as the observed error range is  
230  $\pm 0.4$  ppm for  $^{13}\text{C}$  NMR and  $\pm 0.1$  ppm for  $^1\text{H}$  NMR in methylenes and  $\pm 0.04$  ppm in  
231 methyl and methine groups. The error range has been distinguished on the basis of the  
232 types of hydrogens present in the structure because the methylene assignments are less

233 accurate. In this case, the determination was indirect through the use of two-dimensional  
234 experiments and because the rings A and B methylenes are significantly influenced by  
235 the nature of the sugar chain.

236 Axial and equatorial orientations in the methylene groups are not usually described and  
237 therefore they are defined as 'a' and 'b' in increasing order of chemical shift. In the case  
238 of assignment, the axial positions are generally more shielded than the equatorial ones.  
239 The spatial arrangement of ring A/B is described in the discussion section for those  
240 cases where it has been reported in the bibliography and is of interest.

241 Steroidal-type saponins are the most widely represented structures belonging to *Agave*  
242 species.<sup>16</sup> On the one hand, the structural features included are a spirostane or furostane  
243 backbone and chiral centers at C-5 and C-25. On the other hand, the following  
244 functional groups are also considered, double bonds at C-5, C-9(11) and C-25(27),  
245 hydroxyl groups either in an  $\alpha$  disposition at C-2, C-6 and C-23 or  $\beta$  disposition at C-2,  
246 C-12 and C-24, and finally the presence or absence of a carbonyl group at C-12.

247 The stereochemistry of hydroxylated positions is the same in most cases. Epimers at  
248 these positions are unusual in the *Agave* genus and the revision of some structures is  
249 needed. For example, it was reported that the epimer with a hydroxyl group in a  $\beta$   
250 orientation at C-23 from *Agave fourcroydes*<sup>44</sup> had also been described from *A.*  
251 *cantala*.<sup>32</sup> Nevertheless, it was confirmed that this saponin had the hydroxyl group in an  
252  $\alpha$  orientation rather than  $\beta$ . Moreover, the epimer with a hydroxyl group in the  $\beta$   
253 orientation at C-6 was found in *A. cantala* and its structural elucidation showed that the  
254 aglycone was chlorogenin. However, the hydroxyl group in this saponin is in an  $\alpha$   
255 orientation. These facts confirm that some structures need to be reviewed.

256 Saponins that are representative of those with specific structural characteristics in the  
257 aglycone core have been selected to discuss the most relevant and diagnostic NMR  
258 spectroscopic features. The chemical shifts are within the error range determined as  
259 valid for this review. Sugar moieties bonded at C-3 have direct influence at positions on  
260 ring A to a greater or lesser extent. As a consequence, a greater range of error will be  
261 allowed when describing the influence on the chemical shifts of that ring.

### 262 **2.1. Positions of $^1\text{H}$ and $^{13}\text{C}$ chemical shifts for ring F depending on the C-25** 263 **configuration**

264 Although the changes are not huge in the aglycone structure or backbone of steroidal  
265 saponins reported from the *Agave* genus, some minor variations may considerably  
266 hinder the correct elucidation of this structure. This is the case for the configuration at  
267 C-25 of ring F, which could be defined not only as R or S but also as part of a double  
268 bond with C-27 (Figure 2).

269 Configuration R is, however, the most common within this genus of plants. For this  
270 reason, based on those saponins<sup>45</sup> (**1–3**) with tigogenin as the aglycone (**I**, Table 1), the  
271 influence of the C-25 configuration changes over adjacent carbon positions could be  
272 easily highlighted (Figure 2, Table 3). When C-25 has the S configuration, as in  
273 compound **24**,<sup>46</sup> an upfield shift occurs for the carbon chemical shifts within ring F  
274 (Figure 2), especially for C-25 and C-23, which are shifted upfield by 3.1 ppm and 5.2  
275 ppm, respectively.

276 The  $^1\text{H}$  NMR spectra also show chemical shift variations in ring F when C-25 is S. This  
277 configuration leads to a downfield shift of around 0.37 ppm for the methyl group at C-  
278 27, as well as greater separation of  $\delta_{\text{H}}$  for pairs of geminal protons in methylenes at C-  
279 23, 24, and 26, which is presumably caused by the axial orientation of methyl 27. Such

280 a separation has provided the basis for the well-known Agrawal's rule, which is  
281 currently used to predict the configuration at C-25 with the  $\Delta\delta_{\text{H}}$  of 2H-26.<sup>35,43</sup> It is worth  
282 mentioning that despite a change in the C-25 configuration from R to S, the  $\delta_{\text{H}}$  of H-25  
283 remains unaltered. A slight influence has also been observed on the  $^1\text{H}$  resonance for the  
284 methyl at C-21 when C-25 is S, which usually appears 0.04 ppm upfield. While this  
285 small variation could be within the error considered in this report, it has been regularly  
286 observed when spectra were acquired under the same conditions.

287 Thirdly, when there is a double bond between C-25 and C-27 (**11**),<sup>47</sup> an obvious  
288 downfield shift occurs for the now allylic protons at C-24 and C-26. The signals in  $^1\text{H}$   
289 NMR spectra appear with chemical shift values higher than 2.2 ppm or 4 ppm for  $\text{CH}_2$ -  
290 24 and 26, respectively, relative to the 25R derivative (**1**).

## 291 **2.2. Substitution at C-23 and C-24 of the ring F**

292 Methylene protons at positions C-23 and C-24 of ring F in spirostanoic saponins from the  
293 *Agave* genus are often substituted with hydroxyl groups. In both cases the hydroxyl  
294 group is oriented equatorially, with the one at C-23 being a free hydroxyl group whereas  
295 that at C-24 is usually glycosylated with a glucopyranose moiety (Figure 2).

296 Given that all of the saponins with such substitution patterns isolated to date from  
297 *Agave* genus show a relative R configuration at C-25 (when C-24 is oxygenated the  
298 absolute configuration of C-25 is S), a convenient model to compare and highlight  
299 resonance changes is again tigogenin (**I**). When substituted, the  $\delta_{\text{C}}$  values for the C-23  
300 and C-24 now appear at 67.5 ppm (**58**) and 81.5 ppm (**62**), respectively,<sup>48,49</sup> in the  $^{13}\text{C}$   
301 NMR spectra. It may be that both positions are substituted in a given compound and, in  
302 this case, their  $\delta_{\text{C}}$  are obviously shifted downfield, which is caused by a deshielding  
303 effect of the neighboring electronegative oxygen (Table 3). In  $^1\text{H}$  NMR spectra,

304 however, the methine proton chemical shifts are slightly modified when both C-23 and  
305 C-24 are substituted. Similarly, the carbon chemical shift of C-22, a characteristic  
306 spirostane carbon, is usually shifted downfield by 2.4 ppm when only C-23 is  
307 oxygenated, while this shift increases to 3.4 ppm when C-24 is also substituted. In the  
308 situation where both C-23 and C-24 are oxygenated, the  $\delta_C$  for C-26 (Table 3) is  
309 affected in an additive way and this is clearly visible for compound **60**<sup>50</sup> when compared  
310 with **58** and **62**.

311 A hydroxyl group at C-23 can also cause an upfield shift of the C-20 signal when  
312 compared to tigogenin (**I**), which may be by 6.0 ppm or 7.3 ppm, as in compounds **58**  
313 and **60**. The opposite effect is observed for  $\delta_H$  of H-20 and H-17, the signals of which  
314 are shifted downfield by 1.07 ppm and 0.08 ppm.

315 Despite the fact that the  $^1H$  and  $^{13}C$  resonance signals for methyl 21 are not greatly  
316 affected by substitutions in ring F, the presence of a glycosidic linkage at C-24 causes  
317 an upfield shift of its  $\delta_H$  by 0.1 ppm. This effect, however, is not visible when  
318 substitution occurs in both positions C-23 and C-24, with the hydroxyl group at C-23  
319 being responsible in this case for the observed chemical shift variations for C-20 and C-  
320 21. This double substitution, on the other hand, may also disturb the local magnetic  
321 fields at C-25 and C-27 and therefore the carbon chemical shifts, with glycosylation at  
322 C-24 being crucial. Instead, in the  $^1H$  NMR spectrum the  $\delta_H$  are additively shifted  
323 downfield by 0.49 ppm (**60**) and 0.52 ppm (**60**) for methine 25 and methyl 27,  
324 respectively.

### 325 **2.3. Spirostane/Furostane C-22**

326 The dioxygenated quaternary carbon at position 22 of aglycones could be found as a  
327 ketal or a hemiketal structure. This carbon is the joint between rings E and F in

328 spirostane saponins, while in furostane compounds ring F is opened to yield a  
329 hemiketal carbon at this position. Such a carbon could be found with its hydroxyl group  
330 substituted by a methoxyl group, which has been reported to be a consequence of the  
331 use of methanol during the purification process.<sup>51</sup> C-26 of furostane saponins is in most  
332 cases glycosylated with a glucopyranose.

333 Although the R configuration at C-25 is the most frequent in saponins isolated from the  
334 *Agave* genus, saponins with an S configuration have also been reported.<sup>16</sup> On this basis,  
335 we will now compare the most significant changes in chemical shifts from the <sup>1</sup>H and  
336 <sup>13</sup>C NMR spectra between spirostane (I) and furostane (V) saponins, and between both  
337 C-25 epimers R (V) and S (VI) of the latter. The methoxyl derivative is also included in  
338 this discussion (44).<sup>51</sup>

339 Furostane saponins present very different <sup>1</sup>H and <sup>13</sup>C NMR spectra than the spirostane  
340 compounds.<sup>42</sup> The <sup>13</sup>C chemical shift represents a significant difference when compared  
341 to spirostane saponins because the glycosylation causes a downfield shift by 8.6 ppm  
342 for the C-26 signal (43) (Table 3).<sup>51</sup> Furthermore, the <sup>13</sup>C NMR signals of C-22 and C-  
343 21 are shifted downfield by 1.4 ppm and 1.6 ppm, respectively, while the C-20 signal  
344 moves upfield by 1.1 ppm.

345 Downfield shifts are generally observed in the <sup>1</sup>H NMR spectra of furostane saponins  
346 from the methine at C-17 to the methyl group at C-27. Indeed, the methyl groups at C-  
347 21 and C-27 typically experience the most significant changes, with changes of 0.27  
348 ppm and 0.29 ppm (43) (Table 3),<sup>51</sup> respectively. It is worth noting that opening of ring  
349 F in furostane saponins also induces a slight but consistent downfield shift of the <sup>1</sup>H  
350 NMR signal for the methyl group at C-18 (by 0.05 ppm).



351 The C-25 epimers of furostanoic saponins give rise to very similar  $^{13}\text{C}$  NMR spectra.  
352 However, in the  $^1\text{H}$  NMR spectra there is a downfield shift of methyl-27 for 25R, and  
353 the chemical shift separation between the geminal 2H-26 increases as described by  
354 Agrawal's law.<sup>41,42</sup>

355 In the case where a methoxyl group is attached at C-22, a downfield shift by 2.0 ppm is  
356 observed for this carbon signal (**44**), which is confirmed by the appearance of a new  
357 signal at 47.2 ppm corresponding to the methoxyl group. The opposite effect is  
358 observed for the signal of C-23, which is usually considerably shifted upfield by 6.5  
359 ppm (**44**) (Table 3),<sup>51</sup> with a similar change also observed for methyl 27 (0.4 ppm),  
360 albeit to a lesser extent. In the  $^1\text{H}$  NMR spectrum a methoxyl signal is observed at 3.24  
361 ppm and signals for H-16 to C-24 are mostly shifted upfield with respect to the  
362 hydroxyl derivative (**43**), with changes of 0.08 and 0.14 ppm for the methyl signals H-  
363 18 and H-21.

#### 364 **2.4. Oxygenation at C-12**

365 Several saponins described from the *Agave* genus have a carbonyl group at C-12 (Table  
366 1), while in some other cases this position has been found to be substituted with a  $\beta$ -  
367 hydroxyl group instead. Changes induced by these functionalizations in the neighboring  
368 nuclei are discussed below (Figure 3) and these may serve as diagnostic signals for  
369 structure elucidation.

370 We have noted that a carbonyl group at C-12 of the aglycones may in some way affect  
371 the chemical shifts for all other positions – except for the A and F rings, including when  
372 the latter is opened as in furostanoic saponins. As one would expect, the  $\alpha$ -carbons with  
373 respect to the carbonyl group are the most deshielded (**18**) (Table 4).<sup>48</sup> The carbon  
374 located at a distance of two bonds, namely C-9, is also deshielded but to a lesser extent.

375 An exclusive feature of the *Agave* saponins with a carbonyl group at C-12 is a C-17  
376 signal that is shielded by 8.6 ppm in the  $^{13}\text{C}$  NMR spectra. This signal can be diagnostic  
377 of the presence of a carbonyl group in the molecule (Table 4). Methyl groups at C-21,  
378 C-19 and C-18 are also shielded and the signals move upfield by 1.0 ppm, 0.5 ppm, and  
379 0.4 ppm, respectively.

380 The carbonyl group at C-12 also causes a deshielding effect in the  $^1\text{H}$  NMR spectra.  
381 This is the case for the signals of the methylene group at C-11, which are shifted  
382 downfield by around 1.0 ppm (Table 3). The four methine protons H-8, H-9, H-14 and  
383 H-17 are also shifted downfield (Figure 3) – especially the latter proton, which is  
384 deshielded by 0.95 ppm (**18**) (Table 4).<sup>48</sup> Such an effect is also apparent for  $\delta_{\text{H}}$  of the  
385 methyl groups at C-18 and C-21, the signals of which move by 0.23 ppm and 0.19 ppm,  
386 respectively (**18**).

387 In the furostane saponins from the *Agave* genus that contain a carbonyl group at C-12  
388 (**32**),<sup>10</sup> the  $^1\text{H}$  and  $^{13}\text{C}$  NMR signals of rings D and E seem to be affected by the sum of  
389 the influence of the carbonyl and that of the opened ring F. The positions that show this  
390 additive effect are highlighted in Table 4.

391 When a  $\beta$ -hydroxyl group is attached at C-12 instead of a carbonyl, only the  
392 neighboring carbons (C-11 and C-13) experience a downfield shift of their  $\delta_{\text{C}}$  and this is  
393 by 10.6 ppm and 6.1 ppm, respectively (**47**) (Table 4).<sup>10</sup> The rest of the carbons in ring  
394 C, however, are shielded (Figure 3). In addition, the  $\delta_{\text{C}}$  of the closest methyl group (C-  
395 18) is also shifted upfield, in this case by 5.2 ppm, while the only ring E signals that are  
396 affected are those for C-20 (deshielded, 1.2 ppm) and C-21 (shielded, 0.5 ppm).

397 In the  $^1\text{H}$  NMR spectra of those saponins with a  $\beta$ -hydroxyl group at C-12 (**47**) (Table  
398 4),<sup>10</sup> all  $\delta_{\text{H}}$  from H-9 to H-23a are deshielded to a greater or lesser extent (0.04 ppm to

399 0.44 ppm) (Figure 3). The significant signals of methyl groups at C-18 and C-21 are  
400 shifted downfield by 0.26 ppm and 0.29 ppm, respectively.

#### 401 **2.5. The double bond between C-9 and C-11**

402 In addition to the carbonyl group at C-12, an  $\alpha,\beta$ -unsaturation between C-9 and C-11  
403 has been found in some saponins from the *Agave* genus. Such conjugation causes a  
404 shielding effect on the carbonyl carbon (Figure 3), the signal of which is often found 8.4  
405 ppm upfield (**28**) (Table 4).<sup>52</sup>

406 Besides the downfield shift observed for several carbons as a consequence of the  $\alpha,\beta$ -  
407 unsaturated carbonyl group, such as for C-10 (+3.9 ppm), C-8 (+1.8 ppm) and C-13  
408 (+10.8 ppm), the double bond also produces a distortion in the ring and this is  
409 presumably the cause of shielding of C-14 by 3.4 ppm compared to those saponins  
410 without the unsaturation (**18**, **32**). The opposite effect is found for the methyl group at  
411 C-19, the signal of which is downfield shifted by 8.1 ppm (**28**), while the other methyl  
412 at C-18 is shifted upfield by 1.3 ppm (Figure 3).

413 In the <sup>1</sup>H NMR spectra (**29**) (Table 4)<sup>53</sup>, the most affected signals are those for H-8, H-  
414 19, and H-14, when compared to the hecogenin (**VII**) derivative (**18**), and these are  
415 deshielded by 0.97 ppm, 0.17 ppm and 0.71 ppm, respectively. A similar influence is  
416 observed for the rest of the rings in the aglycone.

#### 417 **2.6. Free hydroxyl group at C-6 and its glycosylation**

418 Position 6 of aglycones can also be oxygenated with a hydroxyl group, which is  
419 oriented equatorially and could also be glycosylated<sup>16</sup>. In the case of the free hydroxyl  
420 group,  $\alpha$  positions (one bond) are deshielded in both the <sup>1</sup>H and <sup>13</sup>C NMR spectra  
421 (Figure 4). The chemical shifts of signals in <sup>1</sup>H NMR spectra for H-4ax, H-8, H-9 and

422 H-19 are significantly affected and are deshielded by 0.15 ppm, 0.19 ppm, 0.13 ppm  
423 and 0.06 ppm, respectively (**45**) (Table 5),<sup>44</sup> while  $\delta_C$  for the methyl C-19 is deshielded  
424 by 1.2 ppm (**45**) in the  $^{13}\text{C}$  NMR spectrum. However, positions beyond ring B are not  
425 affected.

426 In cases where the hydroxyl at C-6 is glycosylated, a strong deshielding effect for the  
427 signal of C-6 (by 11.6 ppm, **46**) with regards to **45** is observed in the  $^{13}\text{C}$  NMR spectra  
428 (Table 5).<sup>10</sup> The signals for adjacent carbons are shifted slightly upfield when compared  
429 to those in saponins with a free hydroxyl group at C-6 (**45**). In the  $^1\text{H}$  NMR spectra  
430 those signals belonging to protons with an equatorial orientation, such as the  
431 glycosylation, are the most affected. In this way, signals for C-4<sub>eq</sub> and C-7<sub>eq</sub> are  
432 deshielded and can be found at 3.39 ppm and 2.57 ppm (**46**). Glycosylation does not  
433 affect the signals for axial protons or the C-19 methyl group when compared with **45**.

434 A long-range effect that is observed is the shielding of the signal for H-16 by 0.13 ppm  
435 (**46**) (Table 5), which is added to the influence of H-23 for saponin **58** (Table 3).

## 436 **2.7. The bridgehead methine at C-5: $\alpha$ - or $\beta$ -spirostanes and the double bond** 437 **between C-5 and C-6**

438 Together with C-25, the other stereocenter that may vary its configuration within the  
439 aglycone backbone of saponins reported from the *Agave* genus is C-5. This carbon is a  
440 bridgehead at the junction between rings A and B, and in fact it has only two possible  
441 configurations, i.e., *cis* when H-5 is  $\beta$ -oriented (equatorial) or *trans* when it is  $\alpha$ -  
442 oriented (axial) (Figure 4). In a similar way to C-25, some saponins have also been  
443 reported to have a double bond between C-5 and C-6. As saponins described from  
444 *Agave* plants mostly have H-5 $\alpha$  (**1**) (Table 5),<sup>45</sup> we discuss below the comparison

445 (Figure 4) with those that contain H-5 $\beta$  (**4**)<sup>54</sup> along with those that are unsaturated in C-  
446 5 (**9**).<sup>55</sup>

447 The <sup>13</sup>C NMR signals for rings A and B of those saponins with a *cis* junction between  
448 these two rings are commonly shielded. Such an effect is especially apparent for the  
449 methines at C-5 and C-9 and methylenes at C-1 and C-7, which are shifted upfield by  
450 7.5 ppm, 13.9 ppm, 6.1 ppm and 5.6 ppm, respectively (Table 5).<sup>54</sup> Agrawal described  
451 the C-5, C-7 and C-9 effects<sup>35</sup> by comparison of the aglycones 5 $\alpha$ -spirostan-3 $\beta$ -ol and  
452 5 $\beta$ -spirostan-3 $\alpha$ -ol.<sup>56</sup> It is necessary to note that for saponins of the *Agave* genus the H-  
453 5 $\beta$  saponins found are 5 $\beta$ -spirostan-3 $\alpha$ -ol and C-1 effects are therefore also observed.  
454 The opposite effect is observed for the methyl group at C-19, the signal of which is  
455 strongly deshielded (by 11.7 ppm downfield, **4**).

456 In the <sup>1</sup>H NMR spectra the observed effect is rather a deshielding and the proton signals  
457 of H-3 and H-19 are particularly noteworthy (by 0.40 ppm and 0.22 ppm) (**4**). The *cis*  
458 junction of rings A and B also affects the signals of methines oriented towards the  $\alpha$ -  
459 face beyond these two rings, such as C-14 (+0.07 ppm), C-16 (+0.05 ppm) and C-17  
460 (+0.06 ppm).

461 Finally, the presence of a double bond between C-5 and C-6 produces a strong  
462 downfield shift in positions C-4 and C-19 (Figure 4), although the  $\delta_C$  for the allylic  
463 carbon C-7 is not affected. Significant shielding is experienced by methines at C-8 (-3.4  
464 ppm) and C-9 (-3.8 ppm) in the <sup>13</sup>C NMR spectrum of saponin **9**, which has diosgenin  
465 (**III**) as the aglycone. The opposite effect is observed in the <sup>1</sup>H NMR spectra, where all  
466 signals from rings A and B are deshielded, including the methyl C-19 (0.23 ppm). As is  
467 common in these systems, the most affected signals are those in the axial position for

468 allylic methylenes C-4 and C-7 and for C-9 (signals move by 1.08 ppm, 0.69 ppm and  
469 0.38 ppm) (Table 5).

470 For the H-5 $\beta$  and  $\Delta^5$  saponins from the *Agave* genus with a carbonyl (**22**)<sup>54</sup> and (**26**)<sup>10</sup> or  
471 hydroxyl group (**48**)<sup>47</sup> at C-12, the <sup>1</sup>H and <sup>13</sup>C NMR signals for positions 8 to 18 are  
472 affected by the sum of its influence. The positions that show this additive effect are  
473 highlighted in Table 5.

## 474 **2.8. Hydroxyl group at C-2**

475 A hydroxyl group can frequently be found attached at C-2 and this is always in an  
476 equatorial disposition regardless of whether the saponins are H-5 $\alpha$ , H-5 $\beta$  or  $\Delta^5$  (Figure  
477 5).

478 In this case, we will compare the H-2 hydroxylated derivatives (**35**)<sup>45</sup> (**38**)<sup>54</sup> (**40**)<sup>55</sup> of  
479 saponins with aglycones that have the same H-5 configuration (**I**, **II** and **III**) (Table 6).  
480 As observed in the <sup>13</sup>C NMR spectra, the positions adjacent to the hydroxyl group are  
481 deshielded, as one would expect, and this is more pronounced for C-1. Positions further  
482 away are slightly affected to different extents, perhaps due to spatial relationships  
483 between the new hydroxyl group and positions in rings A and B, particularly for the *cis*  
484 series (**38**)<sup>54</sup> (Figure 5).

485 The most significant difference in the <sup>13</sup>C NMR spectra is observed for the signal of C-  
486 19, which in the H-5 $\beta$  case (**38**)<sup>54</sup> it is unaffected, while a downfield shift by 1.2 ppm or  
487 1.0 ppm is observed for H-5 $\alpha$  (**35**) or  $\Delta^5$  (**40**)<sup>45,55</sup>. In the case of C-5 (Table 6), the  
488 observed effect is characteristic for each kind of structure and a hydroxyl group at C-2  
489 does not affect the chemical shift of C-5 when the ring junction A/B is *trans*.<sup>45</sup>  
490 However, this signal is shielded by 0.5 and 1.0 ppm, respectively, when the ring fusion

491 is *cis* (**38**)<sup>54</sup> or there is a double bond at C-5 (**40**).<sup>55</sup> Shielding is found for the signal of  
492 C-4 for aglycones with H-5 $\alpha$  and  $\Delta^5$  (0.6 ppm and 1.6 ppm), but a downfield shift by 1.3  
493 ppm is observed when H-5 is  $\beta$  (**71**).

494 The <sup>1</sup>H NMR signals for ring A are sensitive to the nature of the sugar chain attached at  
495 C-3, as described in the next section. These signals usually have a large variability, but  
496 deshielding is the most common effect (Figure 5) except for the H-3 signal, which in the  
497 H-5 $\alpha$  (**35**)<sup>45</sup> and  $\Delta^5$  derivatives<sup>55</sup> is shifted upfield by between 0.04 ppm and 0.11 ppm  
498 (Table 6). For H-5 $\beta$  aglycones,<sup>54</sup> on the other hand, this signal is shifted downfield by  
499 0.1–0.14 ppm. The influence extends into ring B to a lesser extent and the signal for H-9  
500 is sensitive to the presence of a hydroxyl group at C-2 (H-5 $\alpha$  and  $\Delta^5$  +0.09 ppm and  
501 +0.07 ppm; H-5 $\beta$  –0.08 ppm).

502 For the 2-hydroxylated saponins described from the *Agave* genus with a carbonyl (**50**),  
503 (**53**), (**55**)<sup>11</sup> or hydroxyl (**61**)<sup>11</sup> group at C-12, the <sup>1</sup>H and <sup>13</sup>C NMR signals of positions 8  
504 to 18 are affected by the sum of these two factors. The positions that show such additive  
505 effects are highlighted in Table 5.

## 506 **2.9. The main glycosylation at C-3**

507 Although unusual, it is possible to find *Agave* saponins with a free hydroxyl group at C-  
508 3. However, such saponins are frequently glycosylated at C-6 and C-24.<sup>16</sup> In any case,  
509 the absence of glycosylation affects the chemical shifts for carbons C-2, C-3, C-4 and  
510 C-5.<sup>35</sup>

511 The influence of the sugar chain attached at C-3 on the signals for rings A and B is  
512 analyzed below by considering a selection of sugar chains containing glucose,  
513 galactose, and also chains that include up to six sugar moieties (Table 2).

514 The sugar chains found to date in *Agave* plants are divided into two groups, namely  
515 those with one or two sugar units (short chain) and those with more than three (long  
516 chain).<sup>16</sup> Short chain saponins with only one sugar unit usually contain glucose or  
517 galactose attached at C-3, while these two monosaccharaides can also be found in a  
518 disaccharide chain with different connections. In most cases for the second group, a  
519 glucopyranosyl-(1-4)-galactopyranosyloxy unit is attached to position C-3, which in  
520 addition may be further branched with other units of glucose, xylose and also  
521 rhamnoses.

522 With the aim of studying the influence of the sugar chain on the chemical shifts for  
523 rings A and B, we have selected a series of saponins that have the same aglycone  
524 moiety and different sugars chains.

525 Saponins with a *cis* junction between rings A and B (H-5 $\beta$  series) usually contain a  
526 chain with up to three sugar units and a wide variety of inter-connection types. In these  
527 cases, it is quite difficult to identify trends since the  $\delta_C$  values for these rings may  
528 change by  $\pm 0.6$  ppm, which is close to the range of error. A consistent downfield shift  
529 by 0.4 ppm for C-3 in different aglycones is observed when the sugar sequence is  
530 formed by a glucose unit 1-4 connected to a galactose (S2C) (**5**, **15**, **22**),<sup>54</sup> or when a  
531 glucose is 1-2 connected to the glucose unit of S2C (S3A) (**4**, **16**),<sup>54</sup> when compared  
532 with glucopyranosyl derivatives (**11**, **20**, **25**, **30**) (Figure 6).<sup>46,47</sup>

533 The variability observed in the <sup>1</sup>H NMR spectra is also within the range of error, which  
534 is usually higher for methylenes at C-1, C-6 and C-7. The signal for proton H-3 is also  
535 affected (upfield shift by 0.06 ppm) by the previously mentioned sugar chains when  
536 compared with glucopyranosyl derivatives (Figure 6). When the sugar chain is longer in



537 terms of the number of units, the protons farthest from H-3 are also affected, as  
538 observed by comparison between sugar chains S2C and S3A (Figure 6).

539 Saponins with a *trans* fusion (H-5 $\alpha$  series) of rings A and B often contain four or more  
540 sugar units (Table 2). The  $^1\text{H}$  and  $^{13}\text{C}$  NMR spectra of these materials show little  
541 variation and this can be considered to be within the margin of error.

## 542 **2.10. Concluding structural remarks**

543 The structural features and functional groups present in saponins from *Agave* spp. have  
544 a strong influence on  $^1\text{H}$  and  $^{13}\text{C}$  NMR chemical shifts at distances of up to four-bonds.  
545 Additionally, in those cases in which there are significant structural changes through  
546 space, these effects can be observed as long-range correlations.

547 Thus, rings C and F are influenced by functionalization at C-22, C-23 and C-12, while  
548 shielding of rings A and B is altered by functional groups at positions C-2, C-5 and C-6.  
549 Moreover, these effects are additive, especially for the combination of oxygenations at  
550 C-12 and other structural characteristics. A hydroxyl group at C-2 on the three saponin  
551 backbones defined by the nature of H-5 (H-5 $\alpha$ , H-5 $\beta$  or  $\Delta^5$ ) has its peculiarities, since  
552 different spatial arrangements are adopted. It is therefore useful to confirm the structural  
553 elucidation and complete assignments performed by NMR spectroscopic techniques in  
554 order to understand these regularities.

555 The most common errors in the assignment of signals in the aglycone core are due to  
556 the complexity of certain regions in the spectra. For example, oxygenated positions,  
557 which give signals between 3 and 5 ppm in the  $^1\text{H}$  NMR spectra and 90 and 60 ppm in  
558  $^{13}\text{C}$ , are overlapped with chemical shifts of the sugar moiety. The affected signals of the  
559 aglycone skeleton are those at the C-2, C-3, C-6, C-12, C-23 and C-24 positions.<sup>57</sup> In

560 contrast, methylene signals of the aglycone backbone usually appear upfield (below 3  
561 ppm and 50 ppm in  $^1\text{H}$  and  $^{13}\text{C}$  NMR spectra, respectively). HETCOR or HSQC  
562 experiments are used for the structural elucidation of these positions, although it should  
563 be noted that these signals are overlapped, which can result in errors in the assignment<sup>58</sup>  
564 or the determination of only one of the methylene signals in the  $^1\text{H}$  NMR spectrum.

565 TOCSY and HSQC-TOCSY experiments<sup>55</sup> are used in order to achieve an unambiguous  
566 structure elucidation and signal assignment. These techniques allow the assignment of  
567 overlapping signals because they are in a spin system with sufficient deshielded signals  
568 to distinguish their correlations easily.

569 In some cases, a knowledge of patterns allows us to propose the revision of assignments  
570 or structures described in the bibliography. The NMR data for some described structures  
571 are consistent with those previously reported for  $^{13}\text{C}$  NMR spectra, but the  $^1\text{H}$  NMR  
572 chemical shifts differ significantly, even in the case of the methyl signals.<sup>59</sup> A  
573 significant example is the saponin described from *Hosta plantaginea*,<sup>60</sup> which has an  
574 aglycone skeleton that is included in this paper. The authors proposed an  $\alpha,\beta$ -  
575 unsaturated ketone on ring C as a functional group of the aglycone **XI**. Although the  $^{13}\text{C}$   
576 NMR data are in accordance with the signals reported previously,<sup>52</sup> the key  $^1\text{H}$  NMR  
577 chemical shifts (for instance H-11 at 5.87 ppm or H-21 at 1.33 ppm) are not consistent  
578 with the proposed structure. In fact, the chemical shift of the methyl group at H-21 is  
579 affected by the conjugation of the carbonyl group at C-12. This methyl signal shows  
580 values between 1.32 and 1.34 ppm when it is not in conjugation or in the range from  
581 1.41 to 1.39 ppm when it is conjugated (Table 7).<sup>10,52,53</sup>

582 The steroidal saponin described from *Agave attenuata*<sup>61</sup> has sarsapogenin (25S-5 $\beta$ -  
583 spirostanol) as the aglycone. The spectroscopic data for the C-19 position are in

584 agreement with an H-5 $\beta$  disposition, but the rest of the  $^{13}\text{C}$  NMR chemical shifts of  
585 rings A and B are very diverse and they do not have the characteristic shielding data for  
586 H-5 $\beta$  in relation to H-5 $\alpha$ -spirostanes (see section 2.7). Moreover, the structural  
587 elucidation was carried out by comparison of  $^{13}\text{C}$  NMR data of saponinins.<sup>40</sup> Therefore,  
588 a further confirmation of the chemical structure through the use of two-dimensional  
589 NMR experiments is suggested in this case.

### 590 3. IDENTIFICATION OF SAPONINS USING $^1\text{H}$ NMR AND HMBC SPECTRA

591 The comprehensive study of the effects that functional groups and structural  
592 characteristics have on the aglycone signals in the  $^1\text{H}$  and  $^{13}\text{C}$  NMR spectra of *Agave*  
593 saponins indicated that signals are affected up to four bonds away, while changes in  
594 signals that are further away lie within error. Full assignment of signals in the  $^{13}\text{C}$  NMR  
595 spectrum has been performed for the last 35 years and these data have been reported for  
596 all saponins. Regarding  $^1\text{H}$  NMR spectra, the signals for methyl groups have also been  
597 widely described. Assignment of the rest of the signals has been possible with the aid of  
598 high resolution instruments, including the use of multidimensional and selective  
599 excitation experiments. However, the signals due to methylene groups have a larger  
600 range of error.

601 Most of the functionalization found in saponins from *Agave* plants are up to four bonds  
602 away from protons of methyl groups. For this reason, we propose the use of  $^1\text{H}$  NMR  
603 and HMBC spectra only for aglycone identification when the saponin is pure or is  
604 present in a non-complex mixture.

605 The signals of methyl groups in  $^1\text{H}$  NMR spectra are easily visible due to their high  
606 intensity (three equivalent protons). In the case of *Agave* saponins two methyl singlets  
607 ( $\text{CH}_3$ -18 and -19) and two doublets ( $\text{CH}_3$ -21 and -27) are observed, except for those

608 derivatives with a double bond between C-25 and C-27, which are easily recognizable  
609 by the presence of two broad singlets (4.76 and 4.79 ppm).

610 The HMBC spectrum allows correlations to be observed through distances of two and  
611 three bonds from methyl groups. The main advantage of using this technique is that one  
612 can use as references the signals with a less ambiguous assignment since these are the  
613 best described in the literature. In addition, smaller amounts of sample are required for  
614 acquisition when compared to a good quality  $^{13}\text{C}$  NMR spectrum. Furthermore, with  
615 predictive techniques such as NUS<sup>62</sup> it is possible to find the optimal time for the  
616 spectrum acquisition that guarantees its use for the study and even quantification of  
617 saponins.

618 The method described below for the identification of saponins from *Agave* plants could  
619 also be applied for other genera with saponins with the same structural features. The  
620 method begins with the methyl groups (singlets and doublets) as reference signals,  
621 without the need to assign each signal, from which correlations can be observed in the  
622 HMBC spectrum that help to distinguish specific structural features.

### 623 **3.1. HMBC correlations of methyl doublets**

624 The methyl doublets ( $\text{CH}_3$ -21 and -27) typically present correlations with signals from  
625 26 ppm up to 113 ppm (Table 7). This latter signal belongs to C-22 (109-113 ppm),  
626 three bonds away from methyl-21, and may be used for the rapid distinction of methyl-  
627 21. On the other side of the range can be found C-24, with its resonance below 30 ppm  
628 for those saponins without functionalization in ring F (spirostanic or furostanic). For the  
629 doublet of methyl-27, the 25R-spirostanic saponins present a more shielded H-27 signal  
630 than the rest, with a  $\delta_{\text{H}}$  of less than 0.80 ppm. That signal appears close to 1 ppm in  
631 furostanic and 25S-spirostanic saponins and between them it is easy to recognize a

632 correlation with C-26 at  $\delta_C$  75.3 or  $\delta_C$  65.2, respectively. Given that C-23 is four bonds  
633 away from C-21 and C-27, the presence of a hydroxyl group at C-23 can be determined  
634 based on a correlation between H-27 and C-24 (38.9 ppm). In order to determine the  
635 presence of a glucopyranosyloxy group at C-24, the three-bond correlation with this  
636 methyl doublet is useful. Methyl-27 shows a three-bond correlation with a carbon at  
637 81.5 ppm or at 87.9 ppm when C-23 is also hydroxylated.

638 The doublet signal for the methyl group at C-21 is more deshielded than that of C-27,  
639 usually by between 1.0 ppm and 1.6 ppm, and it is very easy to distinguish due to its  
640 HMBC correlation with the signal of C-22 (109–113 ppm).

641 The structural features that are most easily recognizable by using an HMBC spectrum of  
642 a saponin is the kind of oxygenation at C-12 (hydroxyl or carbonyl group), furostane or  
643 spirostane nature or a combination of these two. The presence of a carbonyl group at C-  
644 12 causes a strong shielding at C-17 and this may be observed in correlations from  
645 methyl-21, which is crucial for discriminating between the two possible  
646 functionalizations at this position. Methyl-21 also serves to distinguish a methoxylated  
647 furostane saponin, since it has a common three bond correlation with the methoxyl  
648 group (3.24 ppm) on C-22.

649 The methyl-21 signal appears at around 1.4 ppm in the  $^1\text{H}$  NMR spectrum of saponins  
650 with a hydroxyl group or  $\alpha,\beta$ -unsaturated carbonyl group at C-12. Based on its HMBC  
651 correlation with C-17 (hydroxyl group **47**: 63.0 ppm;  $\alpha,\beta$ -unsaturated carbonyl group  
652 **28**: 54.5 ppm) these can be distinguished from each other (Table 7).

653 The carbon signal for C-20 has a value of around 35 ppm only when C-23 is  
654 oxygenated. This may be distinguished from those saponins that also contain  
655 glucosylation at C-24 on the basis of deshielding experienced by C-22 (up to 112.7

656 ppm). The only two types of saponins that have a signal of C-22 at 111.6 ppm are those  
657 with a hydroxyl group at C-23 or C-24. Only in the latter case, however, does the signal  
658 of C-20 have a chemical shift of 42.1 ppm.

### 659 **3.2. HMBC correlations of methyl singlets**

660 With the previous assignment of the C-17 chemical shift, its three bond HMBC  
661 correlation with a three-proton singlet allows the assignment of methyl C-18. Now,  
662 from this methyl it is possible to identify the kind of functionalization at C-12. Thus, the  
663 HMBC correlation with a  $^{13}\text{C}$  signal at 79.3 ppm (**47**), 212.8 ppm (**18**, **32**) or 204.4 (**28**)  
664 can confirm the presence of a hydroxyl, a carbonyl, or an  $\alpha,\beta$ -unsaturated carbonyl  
665 group, respectively (Table 8).

666 Spirostanic saponins with a hydroxyl group at C-23 give a  $^1\text{H}$  NMR signal for methyl  
667 C-18 at 0.96 ppm (**58**). The correlation with the signal of C-17 at around 62 ppm,  
668 together with the absence of correlations with signals above 200 ppm, can confirm such  
669 a structural feature. It is worth mentioning that the glucopyranosyl group at C-24 causes  
670 strong shielding of the methyl-18 signal (**62**: 0.71 ppm) when other functionalization is  
671 not present in ring F. On the other hand, when functionalization is not present on rings  
672 C or F, the C-18 signal is observed in the range from 0.76 ppm to 0.85 ppm and it  
673 differs by 1.0 ppm for the carbon signal of C-17 of spirostanic and furostanic saponins  
674 (**40**: 62.9 ppm; **43**: 63.9 ppm) (Table 8). The rest of the correlations that have not  
675 previously been mentioned, i.e., those with C-13 and C-14, can be grouped into two  
676 ranges between 39.0 ppm and 42 ppm, and between 54 ppm and 57 ppm.

677 As described before, the signal of the angular methyl-19 can be influenced by  
678 functionalization in rings A–C, but also by the nature of the sugar chain attached at C-3.  
679 As described above for methyl-18, several signals between 35 ppm and 46 ppm and

680 between 53 ppm and 55 ppm (C-1, C-5, C-9 and C-10) show HMBC correlations with  
681 methyl-19. The chemical shifts of these signals are significantly influenced by the  
682 presence of functional groups in rings A and B. However, they are rarely observed away  
683 from these ranges and they are therefore not relevant for structure elucidation.

684 The double bond between C-5 and C-6 or between C-9 and C-11 that is usually present  
685 in saponins from *Agave* is three bonds away from methyl-19. In this way, the HMBC  
686 correlations of this methyl singlet with carbon signals at 141.1 ppm (C-5, **9**), or with  
687 that at 171.3 ppm (C-9, **28**), can be used for their assignment.

688 A *cis* junction between rings A and B (H-5 $\beta$ ) gives rise to a strong deshielding of the  
689 methyl-19 signal and in the  $^1\text{H}$  NMR spectrum this signal is in the range between 0.79  
690 and 0.84 ppm. In the case of a *trans* junction (H-5 $\alpha$ ) this methyl-19 signal is at higher  
691 field, except for those compounds with a double bond between C-9 and C-11.

692 The C-6 position is a four-bond  $^1\text{H}$ - $^1\text{H}$  correlation from the methyl group at C-19. When  
693 this position is oxygenated, the HMBC spectrum shows a three-bond correlation  
694 between methyl-19 and C-5 between 50 and 53 ppm (Table 8). The hydroxylation at C-  
695 6 can also significantly deshield the signal of H-4 $_{\text{eq}}$ , which may be found between 3.36  
696 ppm and 3.39 ppm when a sugar chain is also attached at C-3, or at 3.23 ppm if a free  
697 hydroxyl is present at C-6. This effect is easily detectable since the spectroscopic region  
698 where this signal appears is not frequently hindered by overlap with other proton  
699 signals. In this way, a doublet with a coupling constant of 12 Hz is easily visible and is  
700 diagnostic of the aforementioned structural feature.

701 The position C-2 is also a four-bond correlation from methyl C-19 and its presence  
702 causes appreciable deshielding of the resonance for the C-1 position. Its correlation is  
703 found between 35 and 46 ppm in the HMBC spectrum and the overlap of several signals

704 can also be observed (Table 8). This deshielding makes it easier to distinguish between  
705 saponins that are hydroxylated (**38**, 40.5 ppm)<sup>54</sup> and non-hydroxylated (**4**, 30.8 ppm)<sup>54</sup>  
706 at the C-2 position for H-5 $\beta$  saponins (Table 8). Furthermore, a downfield shift for C-5  
707 of 1 ppm can be readily observed for saponins with a double bond between C-5 and C-  
708 6,  $\Delta^5$  (**9**: 141.1 ppm<sup>55</sup>; **40**, **43**, **44**, **62**: 140.1 ppm<sup>49,51,55</sup>) (Table 8). On the other hand, the  
709 methyl group C-19 is influenced by the C-2 hydroxyl group, as observed in the <sup>1</sup>H  
710 NMR spectrum. Nevertheless, the downfield shift produced for the C-19 singlet is close  
711 to the error range and it is also very sensitive to the sugar chain chemical shifts. Most of  
712 the H-5 $\alpha$  saponins found in *Agave* spp. have a sugar chain with three or more units,  
713 which include a galactose bonded at the C-3 position (Table 2). The anomeric proton in  
714 the <sup>1</sup>H NMR spectrum is not overlapped with other signals in the range from 4.81 ppm  
715 to 4.88 ppm when there is no functional group at the C-2 position (**1-3**, **18**, **47**).<sup>45,48</sup>  
716 However, when there is a hydroxyl group this value is between 4.89 and 4.92 ppm (**35**,  
717 **50**, **51**, **55**, **61**).<sup>10,45</sup> All of these considerations – together with the corresponding  
718 HMBC correlations reported for methyl at C-19 (Table 8) – can indicate the presence or  
719 absence of a hydroxyl group at C-2 on the 5 $\alpha$ -spirostanol core.

### 720 **3.3 Flowchart for the HMBC Method for aglycone identification (HMAI).**

721 Two flowcharts (Figures 7 and 8) are proposed as a tool for the identification of  
722 aglycones of saponins from the *Agave* species (Table 1) by <sup>1</sup>H NMR and HMBC  
723 experiments. Priority has been given to <sup>13</sup>C NMR signals for the detection of structural  
724 features due to their lower sensitivity to the solvent and the nature of the sugar moiety  
725 linked at C-3 when compared to methyl resonances in <sup>1</sup>H NMR spectrum.

726 Both ranges of chemical shifts and absolute values are provided in the flowchart. In this  
727 last case, values within the error range established for this work for <sup>1</sup>H and <sup>13</sup>C NMR



728 signals should be considered. Spectra should be referenced to deuterated pyridine (7.55  
729 ppm and 135.6 ppm for  $^1\text{H}$  and  $^{13}\text{C}$  NMR, respectively).

730 Prior assignment is not needed and only proton signals (for three equivalent protons)  
731 should be distinguished between 1.6 ppm and 0.5 ppm. These signals are readily  
732 recognizable and correspond to secondary methyl groups at C-21 and C-27, which are  
733 doublets and singlets for angular methyl groups C-18 and C-19. The flowchart should  
734 be started with the methyl doublets that provide information on rings C–F. If only one  
735 doublet is observed it is verified that the aglycone contains a double bond at C25(27),  
736 while if two doublet methyl signals are observed it is the doublet that is more deshielded  
737 that is analyzed first (usually C-27).

738 Secondly, methyl groups that give rise to singlets should be investigated and the most  
739 deshielded position will be applied in the flowchart (Figure 8) to assign each methyl  
740 group. In the case of the methyl at C-18, signals from HMBC experiments mainly  
741 provide structural information about ring C and this should be identical to the data  
742 obtained in the study of the methyl group doublets.

743 In some cases, the flowchart indicates that HMBC values for a specific methyl should  
744 be revised. In this situation, taking into consideration the structural features of the  
745 remaining methyls, Tables 7 and 8 should be used.

746 In a case where the HMBC signals are different to those indicated in the flowchart, the  
747 saponin should have other structural characteristics that will require elucidation.

748 A representative example for the application of a saponin in the flowchart is described  
749 below (Figure 9). More examples with structural features included and excluded from  
750 this study are provided in the supporting information.

751 A  $^1\text{H}$  NMR spectrum contains two doublet signals for three equivalent protons at 1.16  
752 ppm and 0.72 ppm. The most deshielded doublet has HMBC correlations with the  
753 signals at 31.9, 38.9 and 66.0 ppm. As the signal did not show correlations with values  
754 lower than 30 ppm (D1-Figure 7) or in the range 109–113 (D5-Figure 7), 88 ppm (D11)  
755 and 81 ppm (D12), it is verified that it has a correlation at approximately 39 ppm (D13),  
756 specifically at 38.9 ppm. This indicates that the methyl analyzed is found at C-27 of a  
757 25R-spirostanic-type saponin and it possesses a hydroxyl group in an  $\alpha$  disposition at C-  
758 23. The second methyl doublet at 1.16 ppm in the  $^1\text{H}$  NMR spectrum has HMBC  
759 correlations with 35.9, 62.6 and 111.7 ppm and these correlations do not fit premise D1.  
760 Nonetheless, a correlation is observed between 109 ppm and 113 ppm (D5-Figure 7),  
761 the characteristic chemical shift of the C-22 position in the  $^{13}\text{C}$  NMR spectrum. This  
762 may confirm that this doublet corresponds with the C-21 position. Moreover,  
763 correlations at 54–55 ppm (D6) and approximately 109 ppm (D9) are not observed.  
764 Thus, by following the indications established in the flowchart, spectroscopic data for  
765 C-21 should be compared with those listed in Table 7 (D10). Comparison of the  
766 shielding data confirms that this compound is a 25R-spirostanic-type saponin with a  
767 hydroxyl group in an  $\alpha$  disposition on C-23 (**58**).

768 The application of the flowchart to the methyl singlets is described in more detail below  
769 (Figure 8). The most downfield shift at 0.96 ppm in the  $^1\text{H}$  NMR spectrum shows  
770 HMBC correlations with signals at 41.0 ppm, 56.5 ppm and 62.6 ppm. Since it does not  
771 have any correlation with values higher than 70 ppm, premises from S1 to S8 are  
772 discarded (Figure 9). On the other hand, a correlation at 62.6 ppm fits with premises S9  
773 and S11 (Figure 8) and therefore this singlet is due to the methyl group at C-18. The  
774 HMBC connectivity data are consistent with those reported for a 25R-spirostanic-type  
775 saponin with a hydroxyl group in an  $\alpha$  orientation at C-23 (**58**, Table 8). It is worth

776 highlighting that the two connectivities that should appear at 40.5 ppm (C-12) and 41.4  
777 ppm (C-13) are overlapped and they are observed as a single signal at 41.0 ppm. The  
778 second methyl singlet (0.74 ppm) corresponds with the C-19 position on the aglycone  
779 skeleton and it shows multiple-bond  $^1\text{H}$ - $^{13}\text{C}$  connectivities at 37.2 ppm, 51.4 ppm and  
780 53.9 ppm. As in the case of the methyl group at C-18, correlations with values higher  
781 than 70 ppm are not observed, although correlations with values higher than 50 ppm are  
782 found (S9-Figure 8). Moreover, there are no correlations with chemical shifts greater  
783 than 60 ppm (S11) but there are between 50 ppm and 52.5 ppm (S13). Besides, the  
784 presence of a doublet signal at 3.23 ppm and a coupling constant of 12 Hz in the  $^1\text{H}$   
785 NMR spectrum (S14) confirms an aglycone with a glucopyranosyloxy group linked to  
786 C-6 and a free hydroxyl group at the C-3 position. These structural features led us to  
787 identify this aglycone as 25R-spirostane-3 $\beta$ ,6 $\alpha$ ,23 $\alpha$ -triol (**XXVI**, Table 1).

788 The example explained below is a mixture of saponins with the same sugar moiety  
789 bonded at C-3 on the aglycone core. Singlet and doublet signals can be observed in the  
790  $^1\text{H}$  NMR spectrum. Some of these signals are overlapped because the differences  
791 between these are far from the methyl groups under study. Doublet signals are observed  
792 between 1.38 ppm and 1.32 ppm along with overlapping regions at around 0.66 ppm,  
793 which could be doublets (Table 9). HMBC correlations (29.2, 30.5 and 66.9 ppm, Table  
794 9) are consistent with the C-27 position (D1-Figure 7). As the H-27 resonance is below  
795 0.80 ppm (D2-Figure 7), 25R-spirostane saponins can be proposed. Other downfield  
796 doublet signals have similar correlations. The signals found at 109.3 ppm or 109.5 ppm  
797 are consistent with them being due to C-21 (D5-Figure 7). Furthermore, the second  
798 correlation at 54.5 ppm or 54.3 ppm (D6-Figure 7) and signals at 109.5 ppm (D7) led us  
799 finally to D8. In this way, it can be determined that a saponin with chemical shift at 1.38

800 ppm in  $^1\text{H}$  NMR spectrum has an  $\alpha,\beta$ -unsaturated carbonyl group at the C-12 position,  
801 while a saponin with proton shielding at 1.32 ppm contains a single carbonyl group.

802 Several singlet signals are found in the  $^1\text{H}$  NMR spectrum. The singlets corresponding  
803 to the C-18 position of each saponin can be distinguished by considering correlations of  
804 C-17, since they are related with the doublet methyl signals at C-21 assigned previously.  
805 A correlation at 54.5 ppm connects the most deshielded doublet (1.38 ppm) with a  
806 singlet at 0.98 ppm. One of the HMBC correlations for this singlet that appears at 204.3  
807 ppm is found within the range established in S3 (204 and 205 ppm, Figure 8). This fact  
808 indicates that there is an  $\alpha,\beta$ -unsaturated carbonyl group at the C-12 position and it  
809 supports the characteristic identified through the correlations of the methyl doublet. The  
810 other two singlet signals, which are very close to each other (1.05 ppm and 1.04 ppm),  
811 share the correlation at 54.2 ppm as overlapped doublets found at 1.32 ppm. There is  
812 also a correlation at 212.7 ppm within the range 212–214 ppm (S1-Figure 8). The  
813 proton chemical shift observed at 1.05 ppm indicates that the spirostane saponins have  
814 a carbonyl group at C-12 (S2-Figure 8), a situation that was already deduced through  
815 the analysis of the corresponding methyl doublet.

816 Overall, it can be stated that the three saponins are 25R-spirostane type with a carbonyl  
817 group at C-12 and that one of them is  $\alpha,\beta$ -unsaturated.

818 The three remaining singlets in the HMBC spectrum correspond to methyl groups at C-  
819 19 (Table 9). The most deshielded methyl group, at 0.80 ppm, shows a correlation with  
820 171.3 ppm, which is in accordance with decision S5. For the third time, it can be  
821 concluded that this saponin has an  $\alpha,\beta$ -unsaturated carbonyl group in ring C and,  
822 furthermore, there is no functionalization in rings A or B and the saponin is H-5 $\alpha$ . The  
823 other two methyl singlets, which belong to aglycones with the same functionalization in  
824 rings C-F, are separated by 0.7 ppm and this suggests that the difference between them

825 is on ring A or B. HMBC correlations for both saponins are very similar and they are  
826 around 55 ppm (S9-Figure 8). Since there are no correlations between 50 ppm and 53  
827 ppm (S11), it can be determined that the A/B ring junction is *trans* for both compounds.  
828 The anomeric proton H-1Gal signal appears below 4.88 ppm and this is related to  
829 saponins without a hydroxyl group at C-2 (S18-Figure 8), although other signals appear  
830 up to 4.88 so there could be some overlapped signal of H-1Gal of a C-2 hydroxylated  
831 derivative. Thus, on comparing the correlations of the two methyl signals at 0.72 ppm  
832 and 0.64 ppm with those previously reported for compounds **35** and **1** (with and without  
833 a hydroxyl group at C-2, respectively) (Table 8), it can be deduced that the most  
834 deshielded signal fits with the presence of a hydroxyl group at C-2, while the most  
835 shielded resonance is due to the absence of further functionalizations in rings A and B.

836 The HMAI method discussed here afforded the assignment of each methyl group for a  
837 mixture of three saponins (Table 9) and identified these aglycones as **VII**, **XI** and **XXII**  
838 (Table 1). It is worth mentioning that methyl doublet and singlet signals are separated  
839 from each other in ranges within the pattern rules established in section 2. For instance,  
840 the methyl at C-19 is particularly affected. This methyl is influenced by the presence of  
841 a hydroxyl group at C-2, which produces a shielding variation of 0.7 ppm (Table 6). In  
842 our study this change was 0.8 ppm for aglycones **VII** and **XXII**. Moreover, a  
843 deshielding of 0.17 ppm is observed if there is an  $\alpha,\beta$ -unsaturated carbonyl group (Table  
844 4). In the aforementioned example, this shielding variation is 0.16 ppm for aglycones  
845 **VII** and **XI**. Additionally, long-range correlations due to the presence of a hydroxyl  
846 group at C-2 are also observed with the C-18 and C-21 signals as a slight shielding  
847 (0.01) which – although within the error range of this study – allows us to distinguish  
848 the two signals (Table 9).

#### 849 4. CONCLUSIONS

850 The pattern rules noted in  $^1\text{H}$  and  $^{13}\text{C}$  NMR spectra for the most representative  
851 aglycones from the *Agave* species indicate that functionalization and structural  
852 modifications produce a shielding variation over a long-range connectivity of up to four  
853 bonds. These effects are usually within the measurement error range at higher multiple-  
854 bond correlation. Besides, the effects are additive and the most influenced signals can  
855 be used to identify structural features. Aglycones can be analyzed through three-bond  
856  $^1\text{H}$ - $^{13}\text{C}$  correlations observed in HMBC experiments for the methyl groups. These  
857 signals are particularly intense and this fact can be used to reduce the acquisition time of  
858 the experiment. Predictive techniques (NUS) can also be used to obtain the desired  
859 correlations in a short time. The chemical shifts for these methyl groups and  $^{13}\text{C}$  NMR  
860 data are usually reported in the bibliography and a spectroscopic data source should be  
861 available to identify other types of saponin.

862 Saponins with a combination of structural requirements, including those evaluated in  
863 this study (Table 1), can be identified through the method for aglycone identification  
864 (HMAI). This method includes a flowchart that facilitates the identification of  
865 aglycones. Besides, the method identifies saponins and proposes structural elucidation  
866 for those that do not fit the premises described. This method has been tested with  
867 HMBC spectra of different saponins and with data reported in the bibliography.  $^{13}\text{C}$   
868 NMR signals are mainly used because they are less influenced by long-range effects or  
869 small variations in deuterated solvents.

870 The application of the HMAI method to a mixture of three saponins allowed the  
871 identification of each aglycone, and it was ascertained that the signals have the same  
872 HMBC correlations as pure saponins within the error range established. Moreover, the  
873 shielding range of the methyl groups in the mixture of saponins fits the patterns  
874 observed in the  $^1\text{H}$  NMR spectra and the results are therefore reinforced.

875 Overall, the HMBC spectrum of methyl signals is proposed as a starting point for the  
876 identification of aglycones from *Agave* saponins. These studies, combined with HPLC-  
877 MS techniques, can be used for quality control or to monitor products that contain  
878 *Agave* saponins.

879

880

881

882

883

#### 884 **ACKNOWLEDGMENTS**

885 This research was supported by the Ministerio de Economía, Industria y Competitividad  
886 (MINEICO), Spain, project: AGL2017-88083-R. The authors are grateful to Juan M.  
887 Calle, Lu Qu, Akihito Yokosuka and Yoshihiro Mimaki for their NMR assignments of  
888 steroidal saponins.

#### 889 **ORCID**

890 Ana M. Simonet                      0000-0002-6516-1783

891 Alexandra G. Durán                0000-0002-9799-0850

892 Andy J. Pérez                        0000-0001-6717-2040

893 Francisco A. Macías                [0000-0001-8862-2864](https://orcid.org/0000-0001-8862-2864)

894

896 **REFERENCES**

- 897 1 Osbourn A. Saponins and plant defence — a soap story. *Trends Plant Sci*  
898 1996;1:4–9.
- 899 2 Hussain M, Debnath B, Qasim M, et al. Role of Saponins in Plant Defense  
900 Against Specialist Herbivores. *Molecules* 2019;24:2067.
- 901 3 Faizal A, Geelen D. Saponins and their role in biological processes in plants.  
902 *Phytochem Rev* 2013;12:877–893.
- 903 4 Yang Y, Laval S, Yu B. Chemical Synthesis of Saponins. In: Horton D, editor.  
904 Advances in Carbohydrate Chemistry and Biochemistry, First edit. London:  
905 Elsevier Inc., 2014. p. 137–226.
- 906 5 Oleszek W, Bialy Z. Chromatographic determination of plant saponins—An  
907 update (2002–2005). *J Chromatogr A* 2006;1112:78–91.
- 908 6 Sparg SG, Light ME, van Staden J. Biological activities and distribution of plant  
909 saponins. *J Ethnopharmacol* 2004;94:219–243.
- 910 7 Wang Y, Zhang Y, Zhu Z, et al. Exploration of the correlation between the  
911 structure, hemolytic activity, and cytotoxicity of steroid saponins. *Bioorg Med*  
912 *Chem* 2007;15:2528–2532.
- 913 8 Yang C-R, Zhang Y, Jacob MR, et al. Antifungal Activity of C-27 Steroidal  
914 Saponins. *Antimicrob Agents Chemother* 2006;50:1710–1714.
- 915 9 Calle JM, Pérez AJ, Simonet AM, et al. Steroidal Saponins from *Furcraea*  
916 *hexapetala* Leaves and Their Phytotoxic Activity. *J Nat Prod* 2016;79:2903–



- 917 2911.
- 918 10 Pérez AJ, Calle JM, Simonet AM, et al. Bioactive steroidal saponins from *Agave*  
919 *offoyana* flowers. *Phytochemistry* 2013;95:298–307.
- 920 11 Pérez AJ, Simonet AM, Calle JM, et al. Phytotoxic steroidal saponins from  
921 *Agave offoyana* leaves. *Phytochemistry* 2014;105:92–100.
- 922 12 Teshima Y, Ikeda T, Imada K, et al. Identification and Biological Activity of  
923 Antifungal Saponins from Shallot (*Allium cepa* L. Aggregatum Group). *J Agric*  
924 *Food Chem* 2013;61:7440–7445.
- 925 13 Mimaki Y, Yokosura A, Kuroda M, et al. Cytotoxic Activities and Structure-  
926 Cytotoxic Relationships of Steroidal Saponins. *Biol Pharm Bull* 2001;24:1286–  
927 1289.
- 928 14 Fujino T, Yokosuka A, Higurashi H, et al. AU-1 from Agavaceae plants causes  
929 transient increase in p21/Cip1 expression in renal adenocarcinoma ACHN cells  
930 in an miR-34-dependent manner. *J Nat Med* 2017;71:36–43.
- 931 15 Fujino T, Yokosuka A, Ichikawa H, et al. AU-1 from Agavaceae plants  
932 downregulates the expression of glycolytic enzyme phosphoglycerate mutase. *J*  
933 *Nat Med* 2018;72:342–346.
- 934 16 Sidana J, Singh B, Sharma OP. Saponins of *Agave*: Chemistry and bioactivity.  
935 *Phytochemistry* 2016;130:22–46.
- 936 17 Cheok CY, Salman HAK, Sulaiman R. Extraction and quantification of saponins:  
937 A review. *Food Res Int* 2014;59:16–40.

- 938 18 Krzyzanowska J, Kowalczyk M, Oleszek W. Analysis of Plant Saponins. In:  
939 Encyclopedia of Analytical Chemistry. Chichester, UK: John Wiley & Sons, Ltd,  
940 2014. p. 1–21.
- 941 19 Urbina CJF, Casas A, Martínez-Díaz Y, et al. Domestication and saponins  
942 contents in a gradient of management intensity of agaves: *Agave cupreata*, *A.*  
943 *inaequidens* and *A. hookeri* in central Mexico. *Genet Resour Crop Evol*  
944 2018;65:1133–1146.
- 945 20 Puente-Garza CA, García-Lara S, Gutiérrez-Urbe JA. Enhancement of saponins  
946 and flavonols by micropropagation of *Agave salmiana*. *Ind Crops Prod*  
947 2017;105:225–230.
- 948 21 Puente-Garza CA, Meza-Miranda C, Ochoa-Martínez D, et al. Effect of in vitro  
949 drought stress on phenolic acids, flavonols, saponins, and antioxidant activity in  
950 *Agave salmiana*. *Plant Physiol Biochem* 2017;115:400–407.
- 951 22 Leal-Díaz AM, Santos-Zea L, Martínez-Escobedo HC, et al. Effect of *Agave*  
952 *americana* and *Agave salmiana* Ripeness on Saponin Content from Aguamiel  
953 (Agave Sap). *J Agric Food Chem* 2015;63:3924–3930.
- 954 23 Puente-Garza CA, Espinosa-Leal CA, García-Lara S. Steroidal Saponin and  
955 Flavonol Content and Antioxidant Activity during Sporophyte Development of  
956 Maguey (*Agave salmiana*). *Plant Foods Hum Nutr* 2018;73:287–294.
- 957 24 Santos-Zea L, Rosas-Pérez AM, Leal-Díaz AM, et al. Variability in Saponin  
958 Content, Cancer Antiproliferative Activity and Physicochemical Properties of  
959 Concentrated Agave Sap. *J Food Sci* 2016;81:H2069–H2075.

- 960 25 Figueroa L, Santos-Zea L, Escalante A, et al. Mass Spectrometry-Based  
961 Metabolomics of Agave Sap (*Agave salmiana*) after Its Inoculation with  
962 Microorganisms Isolated from Agave Sap Concentrate Selected to Enhance  
963 Anticancer Activity. *Sustainability* 2017;9:2095.
- 964 26 Marker RE, Wagner RB, Ulshafer PR, et al. Sterols. CLVII. Sapogenins. LXIX.  
965 1 Isolation and Structures of Thirteen New Steroidal Sapogenins. New Sources  
966 for Known Sapogenins. *J Am Chem Soc* 1943;65:1199–1209.
- 967 27 Wagner RB, Forker RF, Spitzer PF. The  $\Delta^9$ -12-Keto Steroidal Sapogenins. *J Am*  
968 *Chem Soc* 1951;73:2494–2497.
- 969 28 Wilkomirski B, Bobeyko VA, Kintia PK. New steroidal saponins of *Agave*  
970 *americana*. *Phytochemistry* 1975;14:2657–2659.
- 971 29 Sati OP, Rana U, Chaukiyal DC, et al. A New Spirostanol Glycoside from *Agave*  
972 *cantala*. *J Nat Prod* 1987;50:263–265.
- 973 30 Kiyosawa S, Hutoh M, Komori T, et al. Detection of Proto-type Compounds of  
974 Diosgenin-and Other Spirostanol-Glycosides. *Chem Pharm Bull (Tokyo)*  
975 1968;16:1162–1164.
- 976 31 Sharma SC, Sati OP. A spirostanol glycoside from *Agave cantala*.  
977 *Phytochemistry* 1982;21:1820–1821.
- 978 32 Sati OP, Pant G, Miyahara K, et al. Cantalasaponin-1, A Novel Spirostanol  
979 Bisdesmoside from *Agave cantala*. *J Nat Prod* 1985;48:395–399.
- 980 33 Yi D, Yan-Yong C, De-Zu W, et al. Steroidal saponins from a cultivated form of  
981 *Agave sisalana*. *Phytochemistry* 1989;28:2787–2791.

- 982 34 Uniyal GC, Agrawal PK, Sati OP, et al. A spirostane hexaglycoside from *Agave*  
983 *cantala* fruits. *Phytochemistry* 1991;30:4187–4189.
- 984 35 Agrawal PK, Jain DC, Pathak AK. NMR spectroscopy of steroidal sapogenins  
985 and steroidal saponins: An update. *Magn Reson Chem* 1995;33:923–953.
- 986 36 Plock A, Beyer G, Hiller K, et al. Application of MS and NMR to the structure  
987 elucidation of complex sugar moieties of natural products: exemplified by the  
988 steroidal saponin from *Yucca filamentosa* L. *Phytochemistry* 2001;57:489–496.
- 989 37 Yokosuka A, Mimaki Y, Sashida Y. Four New 3,5-Cyclosteroidal Saponins from  
990 *Dracaena surculosa*. *Chem Pharm Bull (Tokyo)* 2002;50:992–995.
- 991 38 Khakimov B, Tseng L, Godejohann M, et al. Screening for Triterpenoid Saponins  
992 in Plants Using Hyphenated Analytical Platforms. *Molecules* 2016;21:1614.
- 993 39 Kim HK, Saifullah, Khan S, et al. Metabolic classification of South American  
994 *Ilex* species by NMR-based metabolomics. *Phytochemistry* 2010;71:773–784.
- 995 40 P. K. Agrawal, D.C. Jain, R. K. Gupta, et al. Carbon-13 NMR Spectroscopy of  
996 Steridal Sapogenins and Steridal Saponins. *Phytochemistry* 1985;24:2479–2496.
- 997 41 Agrawal PK. Assigning stereodiversity of the 27-Me group of furostane-type  
998 steroidal saponins via NMR chemical shifts. *Steroids* 2005;70:715–724.
- 999 42 Agrawal PK. Dependence of <sup>1</sup>H NMR chemical shifts of geminal protons of  
1000 glycosyloxy methylene (H<sub>2</sub>-26) on the orientation of the 27-methyl group of  
1001 furostane-type steroidal saponins. *Magn Reson Chem* 2004;42:990–993.
- 1002 43 Agrawal PK, Burkholz T, Jacob C. Revisit to 25R/25S Stereochemical Analysis

- 1003 of Spirostane-type Steroidal Sapogenins and Steroidal Saponins via  $^1\text{H}$  NMR  
1004 Chemical Shift Data. *Nat Prod Commun* 2012;7:709–711.
- 1005 44 Ohtsuki T, Koyano T, Kowithayakorn T, et al. New chlorogenin hexasaccharide  
1006 isolated from *Agave fourcroydes* with cytotoxic and cell cycle inhibitory  
1007 activities. *Bioorg Med Chem* 2004;12:3841–3845.
- 1008 45 Calle JM. Estudios de fitotoxicidad y relación estructura-actividad (SAR) de  
1009 saponinas esteroidales. Ph. D. Thesis, University of Cadiz, 2015.
- 1010 46 Qu L, Ruan J, Wu S, et al. Separation and Bioactive Assay of 25R/S-Spirostanol  
1011 Saponin Diastereomers from *Yucca schidigera* Roezl (Mojave) Stems. *Molecules*  
1012 2018;23:2562.
- 1013 47 Qu L, Wang J, Ruan J, et al. Spirostane-Type Saponins Obtained from *Yucca*  
1014 *schidigera*. *Molecules* 2018;23:167.
- 1015 48 Pérez AJ. Estudio fitoquímico de especies nativas de Cuba pertenecientes a la  
1016 familia Agavaceae y evaluación de sus actividades biológicas. Ph. D. Thesis,  
1017 University of Cadiz, 2011.
- 1018 49 Mimaki Y, Watanabe K, Sakagami H, et al. Steroidal Glycosides from the  
1019 Leaves of *Cestrum nocturnum*. *J Nat Prod* 2002;65:1863–1868.
- 1020 50 Jin J-M, Zhang Y-J, Yang C-R. Four New Steroid Constituents from the Waste  
1021 Residue of Fibre Separation from *Agave americana* Leaves. *Chem Pharm Bull*  
1022 (*Tokyo*) 2004;52:654–658.
- 1023 51 Macías FA, Guerra JO, Simonet AM, et al. Characterization of three saponins  
1024 from a fraction using  $^1\text{D}$  DOSY as a solvent signal suppression tool.

- 1025 Agabrittonosides E-F. Furostane Saponins from *Agave brittoniana* Trel. spp.  
1026 *Brachypus. Magn Reson Chem* 2010;48: 350-355.
- 1027 52 Mimaki Y, Kanmoto T, Kuroda M, et al. Steroidal Saponins from the  
1028 Underground Parts of *Hosta longipes* and Their Inhibitory Activity on Tumor  
1029 Promoter-Induced Phospholipid Metabolism. *Chem Pharm Bull (Tokyo)*  
1030 1995;43:1190–1196.
- 1031 53 Benito J. Aislamiento biodirigido de saponinas de la especie *Agave americana*.  
1032 Master thesis, University of Cadiz, 2017.
- 1033 54 Yokosuka A, Jitsuno M, Yui S, et al. Steroidal Glycosides from *Agave utahensis*  
1034 and Their Cytotoxic Activity. *J Nat Prod* 2009;72:1399–1404.
- 1035 55 Macías FA, Guerra JO, Simonet AM, et al. Characterization of the fraction  
1036 components using 1D TOCSY and 1D ROESY experiments. Four new spirostane  
1037 saponins from *Agave brittoniana* Trel. spp. *Brachypus. Magn Reson Chem*  
1038 2007;45:615–620.
- 1039 56 Lajis NH, Abdullah ASH, Salim SJS, et al. Epi-Sarsasapogenin and epi-  
1040 smilagenin: two sapogenins isolated from the rumen content of sheep intoxicated  
1041 by *Brachiaria decumbens*. *Steroids* 1993;58:387–389.
- 1042 57 Eskander J, Lavaud C, Harakat D. Steroidal saponins from the leaves of *Agave*  
1043 *macroacantha*. *Fitoterapia* 2010;81:371–374.
- 1044 58 Simmons-Boyce JL, Tinto WF, McLean S, et al. Saponins from *Furcraea selloa*  
1045 var. *marginata*. *Fitoterapia* 2004;75:634–638.
- 1046 59 da Silva BP, Parente JP. A New Bioactive Steroidal Saponin from *Agave shrevei*.

- 1047 *Zeitschrift für Naturforsch C* 2005;60:57–62.
- 1048 60 Wang M, Xu Z, Peng Y, et al. Two New Steroidal Saponins with Antifungal  
1049 Activity from *Hosta plantaginea* Rhizomes. *Chem Nat Compd* 2016;52:1047–  
1050 1051.
- 1051 61 Mendes TP, De Medeiros Silva G, Da Silva BP, et al. A new steroidal saponin  
1052 from *Agave attenuata*. *Nat Prod Res* 2004;18:183–188.
- 1053 62 Xiao H-H, Lv J, Mok D, et al. NMR Applications for Botanical Mixtures: The  
1054 Use of HSQC Data to Determine Lignan Content in *Sambucus williamsii*. *J Nat*  
1055 *Prod* 2019;82:1733–1740.
- 1056 63 Mina S, Melek FR, Abdel-khalik SM, et al. Pharmacological Activities of *Agave*  
1057 *seemanniana* and Isolation of Three Steroidal Saponins. *European J Med Plants*  
1058 2014;4:271–283.
- 1059 64 Zou P, Fu J, Yu H, et al. The NMR studies on two new furostanol saponins from  
1060 *Agave sisalana* leaves. *Magn Reson Chem* 2006;44:1090–1095.
- 1061 65 Yokosuka A, Mimaki Y, Kuroda M, et al. A new steroidal saponin from the  
1062 leaves of *Agave americana*. *Planta Med* 2000;66:393–396.
- 1063
- 1064
- 1065

1066 **Figure legends**

1067 **Figure 1** Representative structure of a steroidal saponin.

1068 **Figure 2**  $^1\text{H}$  and  $^{13}\text{C}$  NMR signals influenced by functionalization at ring F of *Agave*  
1069 saponin aglycones.

1070 **Figure 3**  $^1\text{H}$  and  $^{13}\text{C}$  NMR signals influenced by functionalization at ring C of *Agave*  
1071 saponin aglycones.

1072 **Figure 4**  $^1\text{H}$  and  $^{13}\text{C}$  NMR signals influenced by functionalization at ring B of *Agave*  
1073 saponin aglycones.

1074 **Figure 5**  $^1\text{H}$  and  $^{13}\text{C}$  NMR signals influenced by functionalization at ring A of *Agave*  
1075 saponin aglycones.

1076 **Figure 6**  $^1\text{H}$  and  $^{13}\text{C}$  NMR signals influenced by sugar chains at ring A of *Agave*  
1077 saponin aglycones.

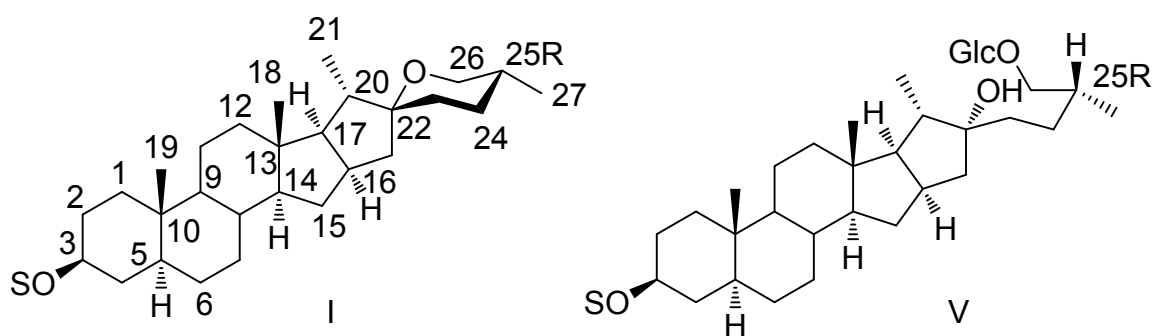
1078 **Figure 7** Flowchart for the HMBC method for aglycone identification (HMAI) of  
1079 saponins from *Agave* species for doublet signals.

1080 **Figure 8** Flowchart for the HMBC method for aglycone identification (HMAI) of  
1081 saponins from *Agave* species for singlet signals.

1082 **Figure 9**  $^1\text{H}$  NMR and HMBC data with representation of HMAI decisions applied.



1084

1085 **Table 1** Saponin aglycones described in this review.

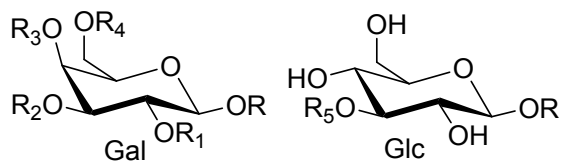
1086

1087

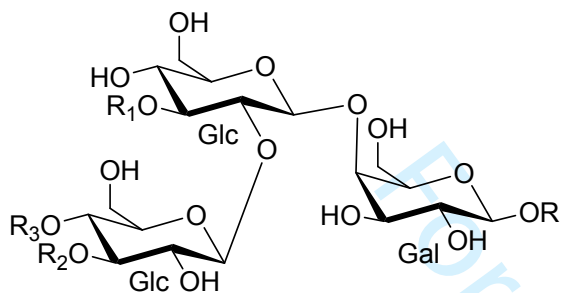
	C-2	C-5	C-6	C-9	C-12	C-23	C-24	C-22	C-25	Saponins
<b>I</b>		$\alpha$						SP	R	<b>1-3</b> <sup>45</sup>
<b>II</b>		$\beta$						SP	R	<b>4-8</b> <sup>45,54</sup>
<b>III</b>		DB						SP	R	<b>9-10</b> <sup>11,55</sup>
<b>IV</b>		$\beta$						SP	DB	<b>11-12</b> <sup>47</sup>
<b>V</b>		$\alpha$						F	R	<b>13-14</b> <sup>63</sup>
<b>VI</b>		$\beta$						F	S	<b>15-17</b> <sup>54</sup>
<b>VII</b>		$\alpha$			CO			SP	R	<b>18-19</b> <sup>48,52</sup>
<b>VIII</b>		$\beta$			CO			SP	R	<b>20-23</b> <sup>46,54</sup>
<b>IX</b>		$\beta$			CO			SP	S	<b>24-25</b> <sup>46</sup>
<b>X</b>		DB			CO			SP	R	<b>26-27</b> <sup>11</sup>
<b>XI</b>		$\alpha$		DB	CO			SP	R	<b>28-29</b> <sup>52,53</sup>
<b>XII</b>		$\beta$			CO			SP	DB	<b>30-31</b> <sup>47</sup>
<b>XIII</b>		DB			CO			F	R	<b>32-33</b> <sup>11</sup>
<b>XIV</b>		DB			CO			F	S	<b>34</b> <sup>64</sup>
<b>XV</b>	OH $\alpha$	$\alpha$						SP	R	<b>35-37</b> <sup>45,52</sup>
<b>XVI</b>	OH $\beta$	$\beta$						SP	R	<b>38-39</b> <sup>54</sup>
<b>XVII</b>	OH $\alpha$	DB						SP	R	<b>40-42</b> <sup>11,55</sup>
<b>XVIII</b>	OH $\alpha$	DB						F	R	<b>43-44</b> <sup>51</sup>
<b>XIX</b>		$\alpha$	OH $\alpha$					SP	R	<b>45-46</b> <sup>11,44</sup>
<b>XX</b>		$\alpha$			OH $\beta$			SP	R	<b>47</b> <sup>48</sup>
<b>XXI</b>		$\beta$			OH $\beta$			SP	DB	<b>48-49</b> <sup>47</sup>
<b>XXII</b>	OH $\alpha$	$\alpha$			CO			SP	R	<b>50-51</b> <sup>10,11</sup>
<b>XXIII</b>	OH $\alpha$	DB			CO			SP	R	<b>52-54</b> <sup>10,11</sup>
<b>XXIV</b>	OH $\alpha$	$\alpha$		DB	CO			SP	R	<b>55-56</b> <sup>10,52</sup>
<b>XXV</b>		$\alpha$	OH $\alpha$		CO			SP	R	<b>57</b> <sup>65</sup>
<b>XXVI</b>		$\alpha$	OH $\alpha$			OH $\alpha$		SP	R	<b>58-59</b> <sup>48</sup>
<b>XXVII</b>		$\alpha$				OH $\alpha$	OH $\beta$	SP	R*	<b>60</b> <sup>50</sup>
<b>XXVIII</b>	OH $\alpha$	DB			OH $\beta$			SP	R	<b>61</b> <sup>10</sup>
<b>XXIX</b>	OH $\alpha$	DB					OH $\beta$	SP	R*	<b>62</b> <sup>49</sup>
<b>XXX</b>		$\alpha$	OH $\alpha$			OH $\alpha$	OH $\beta$	SP	R*	<b>63</b> <sup>50</sup>

1088

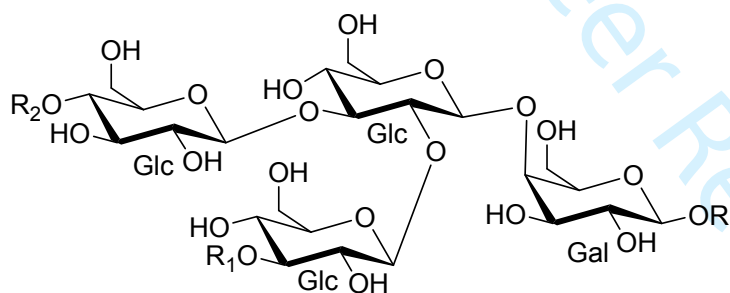
1089 OH: hydroxyl; DB: double bond; CO: carbonyl; SP: spirostanic; F: furostanic; R/S/ $\alpha$ / $\beta$ : chiral center  
 1090 configuration. \*R is the relative configuration.

**Table 2** Sugar chains of saponins described in this review.

Name	R <sub>1</sub>	R <sub>2</sub>	R <sub>3</sub>	R <sub>4</sub>	R <sub>5</sub>
S2A	Glc	H	H	H	
S2B	H	Glc	H	H	
S2C	H	H	Glc	H	
S2D	H	H	H	Glc	
S2E					Glc



Name	R <sub>1</sub>	R <sub>2</sub>	R <sub>3</sub>
S3A	H	H	H
S4A	Xyl	H	H
S5A	Xyl	Xyl	H
S5B	Xyl	Rha	H
S5C	Xyl	Glu	H
S5D	Xyl	H	Rha



Name	R <sub>1</sub>	R <sub>2</sub>
S4B	H	H
S5E	H	Rha
S6A	Glu	Rha

1091

1092 **Table 3** Influence of structure and functionalization of *Agave* saponin aglycons on  $^1\text{H}$  and  $^{13}\text{C}$  NMR  
 1093 chemical shifts. F Ring.

Functionalization of F ring.										
Aglycon	I	IX	IV	XXVI	XXIX	XXVII	XVIII	VI	XVIII	
C-22	SP	SP	SP	SP	SP	SP	F	F	F-OM	
C-23				OH $\alpha$		OH $\alpha$				
C-24					OH $\beta$	OH $\beta$				
C-25	R	S	DB	R	R*	R*	R	S	R	
$^{13}\text{C}$ NMR chemical shifts (ppm. bold numbers) or differences.										
Saponin	<b>1</b>	<b>24</b>	<b>11</b>	<b>58</b>	<b>62</b>	<b>60</b>	<b>43</b>	<b>43</b>	<b>34</b>	<b>44</b>
16	<b>81.0</b>	-1.1 <sup>b</sup>		0.7	0.5	1.0 <sup>a</sup>		<b>81.2</b>		
17	<b>62.9</b>	-8.7 <sup>b</sup>		-0.3	-0.6	-0.9 <sup>a</sup>	1.0	<b>63.9</b>		
20	<b>41.9</b>	1.2 <sup>b</sup>		-6.0		-7.3	-1.1	<b>40.8</b>		
21	<b>14.9</b>	-1.1 <sup>b</sup>					1.6	<b>16.5</b>		
22	<b>109.3</b>	0.5		2.4	2.3	3.4	1.4	<b>110.7</b>		2
23	<b>31.6</b>	-5.2	1.7	<b>67.5</b>	9.2	<b>71.4</b>	5.7	<b>37.3</b>		-6.5
24	<b>29.1</b>	-2.9		9.8	<b>81.5</b>	<b>87.9</b>	-0.6	<b>28.5</b>		
25	<b>30.6</b>	-3.1	<b>144.4</b>	1.2	7.6	7.3	3.8	<b>34.4</b>		
26	<b>66.7</b>	-1.5	-1.7	-0.7	-1.6	-2.6 <sup>a</sup>	8.6	<b>75.3</b>		
27	<b>17.2</b>	-0.9	<b>108.7</b>		-3.7	-4.0 <sup>a</sup>		<b>17.5</b>		-0.4
$^1\text{H}$ NMR chemical shifts (ppm. bold numbers) or differences.										
Saponin	<b>1</b>	<b>24</b>	<b>11</b>	<b>58</b>	<b>62</b>	<b>60</b>	<b>43</b>	<b>43</b>	<b>34</b>	<b>44</b>
16	<b>4.53</b>	-0.04 <sup>b</sup>	0.05				0.38	<b>4.91</b>		-0.50
17	<b>1.77</b>	1.00 <sup>b</sup>	0.06	0.08		0.08 <sup>a</sup>	0.13	<b>1.9</b>		-0.20
18	<b>0.8</b>	0.26 <sup>b</sup>		0.16	-0.09	0.21	0.05	<b>0.85</b>		-0.08
20	<b>1.93</b>	-0.07 <sup>b</sup>		1.07		1.08 <sup>a</sup>	0.27	<b>2.2</b>		
21	<b>1.12</b>	0.23 <sup>b</sup>	-0.04	0.04	-0.10	0.03	0.18	<b>1.3</b>		-0.14
23a	<b>1.62</b>	-0.24	0.14	<b>3.82</b>	0.31	<b>3.84</b>	0.35	<b>1.97</b>		-0.20
23b	<b>1.67</b>	0.13	0.09		0.96		0.34	<b>2.01</b>		
24a	<b>1.54</b>	-0.23	0.68	0.21	<b>4.01</b>	<b>3.96</b>	0.11	<b>1.65</b>		0.13
24b	<b>1.54</b>	0.56	1.15	0.54			0.47	<b>2.01</b>		-0.23
25	<b>1.56</b>			0.24	0.30	0.49 <sup>a</sup>	0.34	<b>1.9</b>		
26a	<b>3.48</b>	-0.13	0.53	-0.04	0.06	0.12	0.11	<b>3.59</b>	-0.11	
26b	<b>3.56</b>	0.46	0.89	-0.04	0.05	0.04	0.36	<b>3.92</b>	0.15	
27a	<b>0.67</b>	0.38	<b>4.76</b>	0.05	0.45	0.52 <sup>a</sup>	0.29	<b>0.96</b>	0.05	
27b			<b>4.79</b>							

1094

1095 OH: hydroxyl; DB: double bond; SP: spirostanic; F: furostanic; R/S/ $\alpha$ / $\beta$ : chiral center configuration. \*R is the relative  
 1096 configuration.

1097 Difference values are obtained from data for ring F. C-25R. spirostanic or furostanic aglycone. Error data:  $^{13}\text{C}$  NMR:

1098  $\pm 0.4$  ppm;  $^1\text{H}$  NMR: methylene signals  $\pm 0.1$  ppm. others  $\pm 0.04$  ppm.

1099 <sup>a</sup> These differences are in agreement with additive effects of C-23 and C-24 hydroxyl groups and <sup>b</sup> additive effects of C-  
 1100 12 carbonyl group and C-25S.

1101

1102

1104 **Table 4** Influence of structure and functionalization of *Agave* saponin aglycones on <sup>1</sup>H and <sup>13</sup>C NMR  
 1105 chemical shifts. C Ring.

Aglycone	Functionalization				
	I	VII	XIII	XX	XI
C-5	α	α	DB	α	α
C-11					DB
C-12		CO	CO	OHα	CO
C-22	SP	SP	F	SP	SP
C-25	R	R	R	R	R
<sup>13</sup> C NMR chemical shifts (ppm, bold numbers) or differences.					
Saponin	<b>1</b>	<b>18</b>	<b>32</b>	<b>47</b>	<b>28</b>
8	<b>35.1</b>	-0.8	-4.2 <sup>b</sup>	-0.7	1.8
9	<b>54.1</b>	1.4	-1.7 <sup>b</sup>	-0.5	<b>171.30</b>
10	<b>35.6</b>	0.7	2.0 <sup>b</sup>		3.9
11	<b>21.1</b>	16.9	16.5	10.6	<b>120.00</b>
12	<b>40</b>	<b>212.8</b>	<b>212.9</b>	<b>79.3</b>	<b>204.30</b>
13	<b>40.5</b>	14.9	14.9	6.1	10.8
14	<b>56.1</b>			-0.9	-3.4
15	<b>32</b>	-0.6	-0.1		
16	<b>81</b>	-1.3	-1.2		-0.8
17	<b>62.9</b>	-8.6	-8.0 <sup>a</sup>		-8.4
18	<b>16.5</b>	-0.4	-0.4	-5.2	-1.3
19	<b>12.2</b>	-0.5	6.7 <sup>b</sup>		6.1
20	<b>41.9</b>	0.7	-0.6 <sup>a</sup>	1.2	1.1
21	<b>14.9</b>	-1.0	0.4 <sup>a</sup>	-0.5	-1.2
<sup>1</sup> H NMR chemical shifts (ppm, bold numbers) or differences.					
Saponin	<b>1</b>	<b>18</b>	<b>32</b>	<b>47</b>	<b>29</b>
8	<b>1.39</b>	0.31	0.42 <sup>b</sup>		0.97
9	<b>0.47</b>	0.38	0.81 <sup>b</sup>	0.15	
11a	<b>1.16</b>	1.02	1.12 <sup>b</sup>	0.31	<b>5.76</b>
11b	<b>1.36</b>	0.97	1.16 <sup>b</sup>	0.44	
12a	<b>1.01</b>			<b>3.48</b>	
12b	<b>1.63</b>				
14	<b>0.99</b>	0.34	0.41 <sup>b</sup>	0.04	0.71
15a	<b>1.38</b>	0.16	0.22	0.17	0.27
15b	<b>2</b>	0.06	0.06	0.07	0.15
16	<b>4.53</b>	-0.08	0.32 <sup>a</sup>	0.07	-0.04
17	<b>1.77</b>	0.95	1.16 <sup>a</sup>	0.38	0.85
18	<b>0.8</b>	0.23	0.33 <sup>a</sup>	0.26	0.19
19	<b>0.62</b>		0.29 <sup>b</sup>		0.17
20	<b>1.93</b>	-0.05	0.26 <sup>a</sup>	0.25	0.05
21	<b>1.12</b>	0.19	0.41 <sup>a</sup>	0.29	0.27

1106

1107 OH: hydroxyl; DB: double bond; CO: carbonyl; SP: spirostanic; F: furostanic; R/S/α/β: chiral center configuration.

1108 Difference values are obtained from data for 25R-spirostanic aglycone. Error data: <sup>13</sup>C NMR: ±0.4 ppm; <sup>1</sup>H NMR:

1109 methylene signals ±0.1 ppm, others ±0.04 ppm.

1110 <sup>a</sup> These differences are in agreement with additive effects of C-12 carbonyl group and furostanic structure and <sup>b</sup> additive

1111 effects of C-12 carbonyl group and C-5 double bond.

1113 **Table 5** Influence of structure and functionalization of *Agave* saponin aglycones on <sup>1</sup>H and <sup>13</sup>C NMR  
 1114 chemical shifts. B Ring.

Aglycone	Functionalization								
	I	XIX	XIX	XI	II	VIII	XXI	III	X
C-5	<i>α</i>	<i>α</i>	<i>α</i>	<i>α</i>	<i>β</i>	<i>β</i>	<i>β</i>	DB	DB
C-6		OH <i>α</i>	OGlc <i>α</i>						
C-9				DB					
C-12				CO		CO	OH <i>β</i>		CO
<sup>13</sup> C NMR chemical shifts (ppm, bold numbers) or differences.									
Saponin	<b>1</b>	<b>45</b>	<b>46</b>	<b>28</b>	<b>4</b>	<b>22</b>	<b>48</b>	<b>9</b>	<b>26</b>
1	<b>36.9</b>			-1.9	-6.1	-6.5	-5.9	0.6	0.1
2	<b>29.8</b>				-2.8	-3.1	-2.9	0.4	0.1
3	<b>78.1</b>			-1.4	-3.4	-3.8	-3.8		
4	<b>34.7</b>	-5.3	-6.1		-4	-4.1	-4.2	4.6	4.4
5	<b>44.4</b>	7.7	6.5	-1.9	-7.5	-7.9	-7.6	<b>141.1</b>	<b>140.9</b>
6	<b>28.8</b>	<b>68.3</b>	<b>79.9</b>	-0.9	-1.8	-2.1	-1.7	<b>121.7</b>	<b>121.5</b>
7	<b>32.3</b>	10.3	9.1		-5.6	-6	-5.6		-0.5
8	<b>35.1</b>	-0.9	-1	1.8	0.4	-0.4 <sup>a</sup>	-0.4 <sup>b</sup>	-3.4	-4.2 <sup>a</sup>
9	<b>54.1</b>			<b>171.30</b>	-13.9	-12.2 <sup>a</sup>	-14.7 <sup>b</sup>	-3.8	-1.8 <sup>a</sup>
10	<b>35.6</b>	0.8	1.1	3.9	-0.4	0 <sup>a</sup>	-0.3 <sup>b</sup>	1.5	2 <sup>a</sup>
14	<b>56.1</b>			-3.4			-0.8 <sup>b</sup>	0.6	
19	<b>12.2</b>	1.2	1.2	6.1	11.7	10.8 <sup>a</sup>	11.6 <sup>b</sup>	7.3	6.7 <sup>a</sup>
<sup>1</sup> H NMR chemical shifts (ppm, bold numbers) or differences.									
Saponin	<b>1</b>	<b>45</b>	<b>46</b>	<b>29</b>	<b>4</b>	<b>22</b>	<b>48</b>	<b>9</b>	<b>26</b>
1a	<b>0.75</b>			0.40	0.69	0.47	0.68	0.18	0.10
1b	<b>1.47</b>				0.32	0.15	0.27	0.18	
2a	<b>1.60</b>				-0.18	-0.25	-0.10	0.08	
2b	<b>2.02</b>				-0.13	-0.23	-0.15	0.07	
3	<b>3.89</b>				0.40	0.35	0.43		-0.08
4a	<b>1.32</b>	0.15	0.12		0.37	0.34	0.40	1.08	1.06
4b	<b>1.77</b>		1.62			-0.07		0.87	0.88
5	<b>0.86</b>	0.31	0.37	0.17	1.19	1.12	1.15		
6a	<b>1.04</b>	<b>3.55</b>	<b>3.59</b>	0.12				<b>5.27</b>	<b>5.25</b>
6b	<b>1.08</b>			0.08	0.63	0.64	0.65		
7a	<b>0.75</b>	0.39		0.12	0.18	0.17	0.20	0.69	0.69
7b	<b>1.48</b>	0.70	1.09	0.23	-0.25	-0.18	-0.17	0.33	0.36
8	<b>1.39</b>	0.19	0.13	0.97	0.07	0.41 <sup>a</sup>	0.13	0.09	0.42 <sup>a</sup>
9	<b>0.47</b>	0.13			0.80	1.24 <sup>a</sup>	0.99 <sup>b</sup>	0.38	0.81 <sup>a</sup>
11a	<b>1.16</b>					1.02 <sup>a</sup>	0.31 <sup>b</sup>	0.19	1.10 <sup>a</sup>
11b	<b>1.36</b>				-0.07	0.98 <sup>a</sup>	0.39 <sup>b</sup>	0.08	1.14 <sup>a</sup>
12a	<b>1.01</b>				0.06		<b>3.51</b>		
12b	<b>1.63</b>								
14	<b>0.99</b>			0.71	0.07	0.44 <sup>a</sup>	0.14 <sup>b</sup>		0.41 <sup>a</sup>
15a	<b>1.38</b>			0.24		0.19 <sup>a</sup>	0.20 <sup>b</sup>		0.20 <sup>a</sup>
15b	<b>2.00</b>			0.15			0.08 <sup>b</sup>		0.08 <sup>a</sup>
16	<b>4.53</b>		-0.13	-0.02	0.05	-0.0 <sup>a</sup>	0.14 <sup>b</sup>		-0.07 <sup>a</sup>
17	<b>1.77</b>			0.85	0.06	1.02 <sup>a</sup>	0.43 <sup>b</sup>		1.01 <sup>a</sup>
18	<b>0.80</b>			0.19		0.26 <sup>a</sup>	0.26 <sup>b</sup>		0.27 <sup>a</sup>
19	<b>0.62</b>	0.06	0.06	0.17	0.22	0.18 <sup>a</sup>	0.22	0.23	0.28

1115 OH: hydroxyl; DB: double bond; CO: carbonyl; SP: spirostanoic; F: furostanoic; R/S/*α*/*β*: chiral center configuration.  
 1116 Difference values are obtained from data for 25R-spirostanic aglycone. Error data: <sup>13</sup>C NMR: ±0.4 ppm; <sup>1</sup>H NMR:  
 1117 methylenes signals ±0.1 ppm, others ±0.04 ppm.

1118 <sup>a</sup> These differences are in agreement with additive effects of C-12 carbonyl group and H-5 $\beta$  or  $\Delta^5$ -spirostanol and <sup>b</sup>  
 1119 additive effects of C-12 hydroxyl group H-5 $\beta$ -spirostanol.

1120

1121 **Table 6** Influence of structure and functionalization of *Agave* saponin aglycones on  $^1\text{H}$  and  $^{13}\text{C}$  NMR  
 1122 chemical shifts. A Ring.

Sugar moiety Aglycon	Functionalization									
	S6A I	S3A XV	S5A XXII	S5A XXIV	S3A II	S3A XVI	S5A III	S5A XVII	S5A XXIII	S4A XXVIII
C-2		OH $\alpha$	OH $\alpha$	OH $\alpha$		OH $\beta$		OH $\alpha$	OH $\alpha$	OH $\alpha$
C-5	$\alpha$	$\alpha$	$\alpha$	$\alpha$	$\beta$	$\beta$	DB	DB	DB	
C-9					DB					
C-12			CO	CO					CO	OH $\beta$
$^{13}\text{C}$ NMR chemical shifts (ppm, bold numbers) or differences.										
Saponin	<b>1</b>	<b>35</b>	<b>50</b>	<b>55</b>	<b>4</b>	<b>38</b>	<b>9</b>	<b>40</b>	<b>53</b>	<b>61</b>
1	<b>36.9</b>	8.7	8.2	6.6 <sup>a</sup>	<b>30.8</b>	9.7	<b>37.5</b>	8.3	7.8	8.3
2	<b>29.8</b>	<b>70.3</b>	<b>70.2</b>	<b>70.3</b>	<b>27.0</b>	<b>79.7</b>	<b>30.2</b>	<b>70.1</b>	<b>69.8</b>	<b>70.0</b>
3	<b>78.1</b>	6.5	5.9	5.4 <sup>a</sup>	<b>74.7</b>	5.0	<b>78.3</b>	6.3	6.0	6.3
4	<b>34.7</b>	-0.6	-0.8	-1.0 <sup>a</sup>	<b>30.7</b>	1.3	<b>39.3</b>	-1.6	-1.8	-1.7
5	<b>44.4</b>			-1.9 <sup>a</sup>	<b>36.9</b>	-0.5	<b>141.1</b>	-1.0	-1.2	-1.0
6	<b>28.8</b>	-0.8	-1.0	-1.6 <sup>a</sup>	<b>27.0</b>	-0.8	<b>121.7</b>			
7	<b>32.3</b>		-0.7		<b>26.7</b>		<b>32.3</b>		-0.6	
8	<b>35.1</b>	-0.6	-1.4 <sup>a</sup>	1.1 <sup>a</sup>	<b>35.5</b>		<b>31.7</b>	-0.6	-1.3 <sup>a</sup>	-1.3 <sup>b</sup>
9	<b>54.1</b>	0.2	1.3 <sup>a</sup>	<b>170.5</b>	<b>40.2</b>	1.2	<b>50.3</b>		1.8 <sup>a</sup>	-0.3 <sup>b</sup>
10	<b>35.6</b>	1.2	2.5 <sup>a</sup>	5.0 <sup>a</sup>	<b>35.2</b>	1.7	<b>37.1</b>	0.9	1.3 <sup>a</sup>	1.0 <sup>b</sup>
19	<b>12.2</b>	1.2	0.7 <sup>a</sup>	7.2 <sup>a</sup>	<b>23.9</b>	-0.1	<b>19.5</b>	1.0	0.4 <sup>a</sup>	1.0 <sup>b</sup>
$^1\text{H}$ NMR chemical shifts (ppm, bold numbers) or differences.										
Saponin	<b>1</b>	<b>35</b>	<b>50</b>	<b>55</b>	<b>4</b>	<b>38</b>	<b>9</b>	<b>40</b>	<b>53</b>	<b>61</b>
1a	<b>0.75</b>	0.37	0.34	0.80 <sup>a</sup>	<b>1.44</b>	0.32	<b>0.93</b>	0.34	0.29	0.35
1b	<b>1.47</b>	0.70	0.53	0.74 <sup>a</sup>	<b>1.79</b>	0.11	<b>1.65</b>	0.64	0.49	0.64
2a	<b>1.60</b>	<b>3.95</b>	<b>3.89</b>	<b>4.00</b>	<b>1.42</b>	<b>3.85</b>	<b>1.68</b>	<b>4.06</b>	<b>3.99</b>	<b>4.00</b>
2b	<b>2.02</b>				<b>1.89</b>		<b>2.09</b>			
3	<b>3.89</b>	-0.05	-0.07	-0.06	<b>4.29</b>	0.14	<b>3.87</b>	-0.06	-0.09	-0.08
4a	<b>1.32</b>	0.15	0.12	0.17	<b>1.69</b>	0.14	<b>2.40</b>	0.13	0.11	0.11
4b	<b>1.77</b>	0.05	0.07	0.14	<b>1.80</b>	0.11	<b>2.64</b>	0.04	0.07	0.05
5	<b>0.86</b>	0.11	0.07	0.29 <sup>a</sup>	<b>2.05</b>	-0.03				
6a	<b>1.04</b>	-0.05		0.19 <sup>a</sup>	<b>1.03</b>	0.03	<b>5.27</b>			
6b	<b>1.08</b>	0.02	0.04	0.08 <sup>a</sup>	<b>1.71</b>	-0.06				
7a	<b>0.75</b>			0.12 <sup>a</sup>	<b>0.93</b>		<b>1.44</b>			
7b	<b>1.48</b>			0.25 <sup>a</sup>	<b>1.23</b>		<b>1.81</b>			
8	<b>1.39</b>		0.31 <sup>a</sup>	0.97 <sup>a</sup>	<b>1.46</b>	-0.04	<b>1.48</b>		0.30 <sup>a</sup>	
9	<b>0.47</b>	0.09	0.49 <sup>a</sup>		<b>1.27</b>	-0.08	<b>0.85</b>	0.07	0.51 <sup>a</sup>	0.25 <sup>b</sup>
11a	<b>1.16</b>	0.02	1.16 <sup>a</sup>		<b>1.16</b>		<b>1.35</b>		1.02 <sup>a</sup>	0.32 <sup>b</sup>
11b	<b>1.36</b>	0.08	1.02 <sup>a</sup>		<b>1.29</b>	0.15	<b>1.44</b>		1.08 <sup>a</sup>	0.49 <sup>b</sup>
19	<b>0.62</b>	0.07	0.08	0.24 <sup>a</sup>	<b>0.84</b>	0.03	<b>0.85</b>	0.06	0.10	0.10

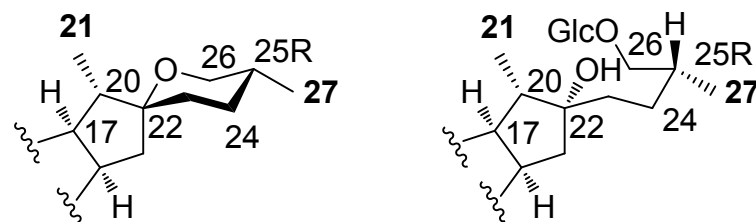
1123

1124 OH: hydroxyl; DB: double bond; CO: carbonyl;  $\alpha/\beta$ : chiral center configuration.

1125 Difference values are obtained from data for aglycones I, II and III. Error data:  $^{13}\text{C}$  NMR:  $\pm 0.4$  ppm;  $^1\text{H}$  NMR:  
 1126 methylene signals  $\pm 0.1$  ppm, others  $\pm 0.04$  ppm.

1127 <sup>a</sup> These differences are in agreement with additive effects of C-12 carbonyl group and spirostan-2,3-diols and <sup>b</sup> additive  
 1128 effects of C-12 hydroxyl group and spirostan-2,3-diols H-5 $\beta$ -spirostanol.

1129 **Table 7** HMBC correlations with doublet signals of methyl groups C-21 and C-27.



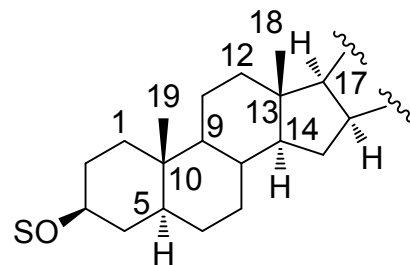
1130

Structural Features						HMBC signals								
C-9	C-12	C-23	C-24	C-22	C-25	H-27	C-24	C-25	C-26	H-21	C-17	C-20	C-22	Data
				SP	R	0.67	29.1	30.6	66.7	1.12	62.9	41.9	109.3	<b>1</b>
				SP	DB	-	-	-	-	1.08	63.2	41.9	109.4	<b>11</b>
				F	R	0.96	28.5	34.4	75.3	1.30	63.9	40.8	110.7	<b>43</b>
				FM	R	0.98	28.2	34.2	75.2	1.16	64.1	40.5	112.7	<b>44</b>
		OH $\alpha$		SP	R	0.72	38.9	31.8	66.0	1.16	62.6	35.9	111.7	<b>58</b>
			OGlc $\beta$	SP	R*	1.12	81.5	38.2	65.1	1.02	62.3	42.1	111.6	<b>62</b>
		OH $\alpha$	OGlc $\beta$	SP	R*	1.19	87.9	37.9	64.1	1.15	62.0	34.6	112.7	<b>60</b>
	CO			SP	S	1.05	26.2	27.5	65.2	1.35	54.2	43.1	109.8	<b>24</b>
	CO			SP	R	0.64	29.2	30.5	66.9	1.31	54.3	42.6	109.3	<b>18</b>
	CO			F	R	0.96	28.4	34.3	75.3	1.53	54.9	41.3	110.9	<b>32</b>
	CO			F	S	1.01	28.3	34.4	75.3	1.51	54.8	41.3	110.8	<b>34</b>
DB	CO			SP	R	0.67	29.2	30.5	67.0	1.38	54.5	43.0	109.5	<b>28</b>
	OH $\beta$			SP	R	0.67	29.4	30.7	66.9	1.41	63.0	43.1	109.6	<b>47</b>

1131

1132 OH: hydroxyl; DB: double bond; CO: carbonyl; SP: spirostane; F: furostane; R/S/ $\alpha$ / $\beta$ : chiral center configuration.

1133 \* R is the relative configuration; S is the absolute configuration because a glucopyranosyloxy moiety is at C-24.

**Table 8** HMBC correlations with doublet signals of methyl groups C-18 and C-19.

Structural Features								HMBC signals										
C-2	C-5	C-6	C-9	C-12	C-22	C-23	C-24	H-18	C-12	C-13	C-14	C-17	H-19	C-1	C-5	C-9	C-10	Data
	$\alpha$				SP			0.80	40.0	40.5	56.1	62.9	0.62	36.9	44.4	54.1	35.6	<b>1</b>
	$\alpha$				SP	OH $\alpha$	OGlc $\beta$	1.01	40.7	41.4	56.6	62	0.75	37.5	45.6	54.6	35.9	<b>60</b>
	$\alpha$			CO	SP			1.03	212.8	55.4	55.9	54.3	0.61	36.6	44.4	55.5	36.3	<b>18</b>
	$\alpha$		DE	CO	SP			0.98	204.3	51.3	52.7	54.5	0.79	35.0	42.5	171.3	39.5	<b>28</b>
OH $\alpha$	$\alpha$		DE	CO	SP			0.97	204.3	51.4	52.7	54.6	0.86	43.5	42.5	170.5	40.6	<b>55</b>
	$\alpha$			OH $\beta$	SP			1.06	79.3	46.6	55.2	63.0	0.64	37.2	44.7	53.6	35.9	<b>47</b>
OH $\alpha$	$\alpha$				SP			0.78	40.0	40.6	56.3	63.0	0.69	45.6	44.6	54.3	36.8	<b>35</b>
	$\beta$				SP			0.79	40.3	40.9	56.5	63.1	0.84	30.8	36.9	40.2	35.2	<b>4</b>
OH $\beta$	$\beta$				SP			0.77	40.2	40.8	56.3	63.1	0.87	40.5	36.4	41.4	36.9	<b>38</b>
	DB				SP			0.80	39.9	40.5	56.7	62.9	0.85	37.5	141.1	50.3	37.1	<b>9</b>
	DB			CO	F			1.13	212.9	55.4	56.0	54.9	0.91	37.0	140.9	52.4	37.6	<b>32</b>
OH $\alpha$	DB				SP			0.78	39.8	40.5	56.5	62.9	0.91	45.8	140.1	50.2	38.0	<b>40</b>
OH $\alpha$	DB				SP		OGlc $\beta$	0.71	39.7	40.4	56.5	62.3	0.91	45.7	140.1	50.1	37.9	<b>62</b>
OH $\alpha$	DB				F			0.85	39.9	40.8	56.5	63.9	0.92	45.8	140.1	50.3	38.0	<b>43</b>
OH $\alpha$	DB				FM			0.77	39.6	40.8	56.4	64.1	0.91	45.7	140.1	50.2	37.9	<b>44</b>
	$\alpha$	OH $\alpha$			SP			0.81	40.0	40.7	56.2	62.9	0.68	37.6	52.1	54.0	36.4	<b>45</b>
	$\alpha$	OGlc $\alpha$			SP			0.76	40.0	40.8	56.4	63.0	0.68	37.5	50.9	53.8	36.7	<b>46</b>
	$\alpha$	OGlc $\alpha$			SP	OH $\alpha$		0.96	22.7	41.4	56.5	62.6	0.74	37.8	51.3	54.0	36.8	<b>58</b>

OH: hydroxyl; DB: double bond; CO: carbonyl; SP: spirostanic; F: furostanic;  $\alpha/\beta$ : chiral center configuration.



2000

2001 **Table 9** HMBC correlations observed for saponin mixture.

2002

<sup>1</sup> H NMR signal	HMBC correlations			Methyl assignment	Aglycone assignment
1.38 d	42.9	54.5	109.5	C-21	<b>XI</b>
1.33 d	42.6	54.3	109.3	C-21	<b>VII</b>
1.32 d	overlapped	overlapped	overlapped	C-21	<b>XXII</b>
1.05 s	54.2	55.5	212.7	C-18	<b>VII</b>
1.04 s	overlapped	overlapped	overlapped	C-18	<b>XXII</b>
0.98 s	51.3	52.6	54.5	204.3 C-18	<b>XI</b>
0.80 s	35.0	39.5	42.5	171.3 C-19	<b>XI</b>
0.72 s	37.2	44.7	55.3	C-19	<b>XXII</b>
0.66 d	29.2	30.5	66.9	C-27	<b>VII; XI; XXII</b>
0.64 s	36.4	44.4	55.5	C-19	<b>VII</b>

2003

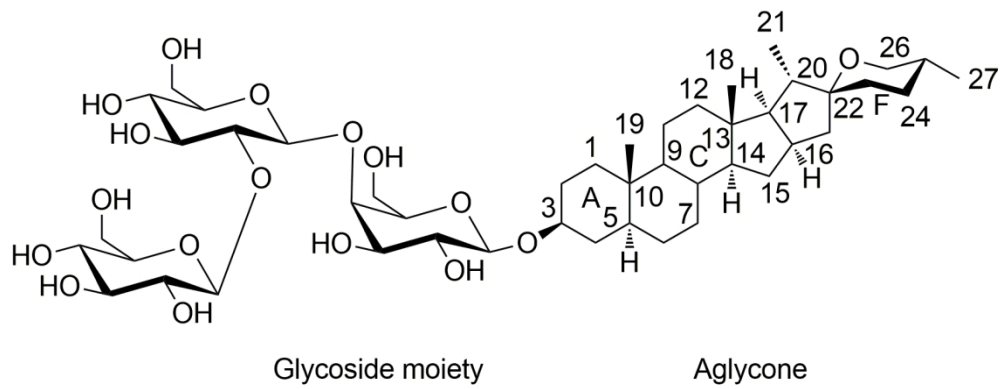


Figure 1 Representative structure of a steroidal saponin.

152x59mm (300 x 300 DPI)

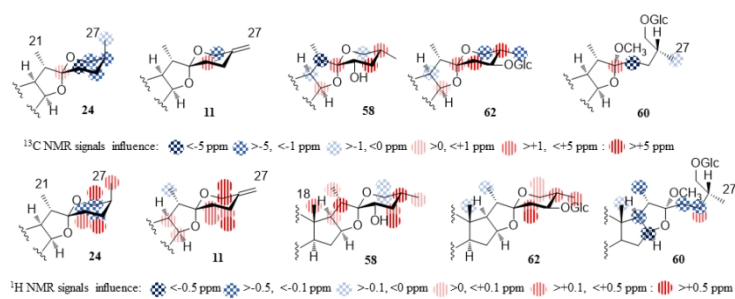


Figure 2 <sup>1</sup>H and <sup>13</sup>C NMR signals influenced by functionalization at ring F of Agave saponin aglycones.

338x190mm (96 x 96 DPI)

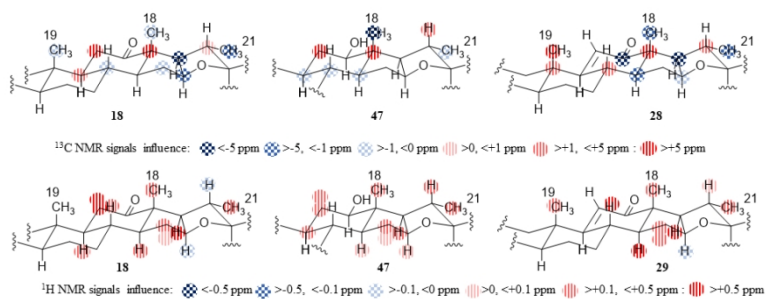


Figure 3 <sup>1</sup>H and <sup>13</sup>C NMR signals influenced by functionalization at ring C of Agave saponin aglycones.

338x190mm (96 x 96 DPI)

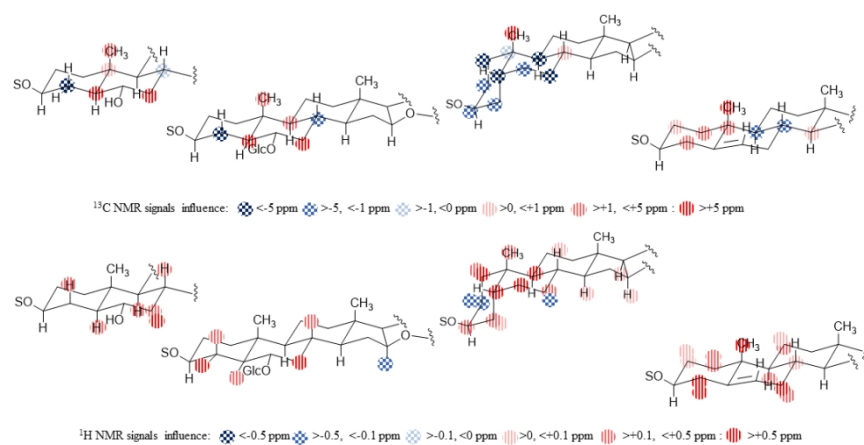


Figure 4 <sup>1</sup>H and <sup>13</sup>C NMR signals influenced by functionalization at ring B of Agave saponin aglycones.

338x190mm (96 x 96 DPI)

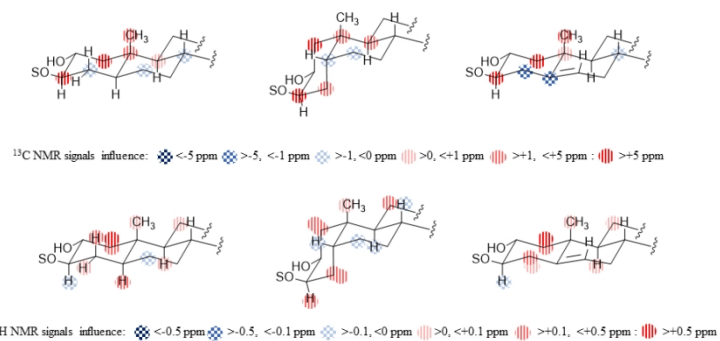


Figure 5 <sup>1</sup>H and <sup>13</sup>C NMR signals influenced by functionalization at ring A of Agave saponin aglycones.

338x190mm (96 x 96 DPI)

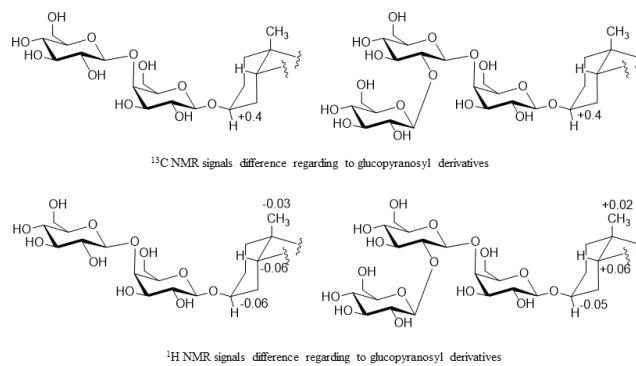


Figure 6  $^1\text{H}$  and  $^{13}\text{C}$  NMR signals influenced by sugar chains at ring A of Agave saponin aglycones.

338x190mm (96 x 96 DPI)

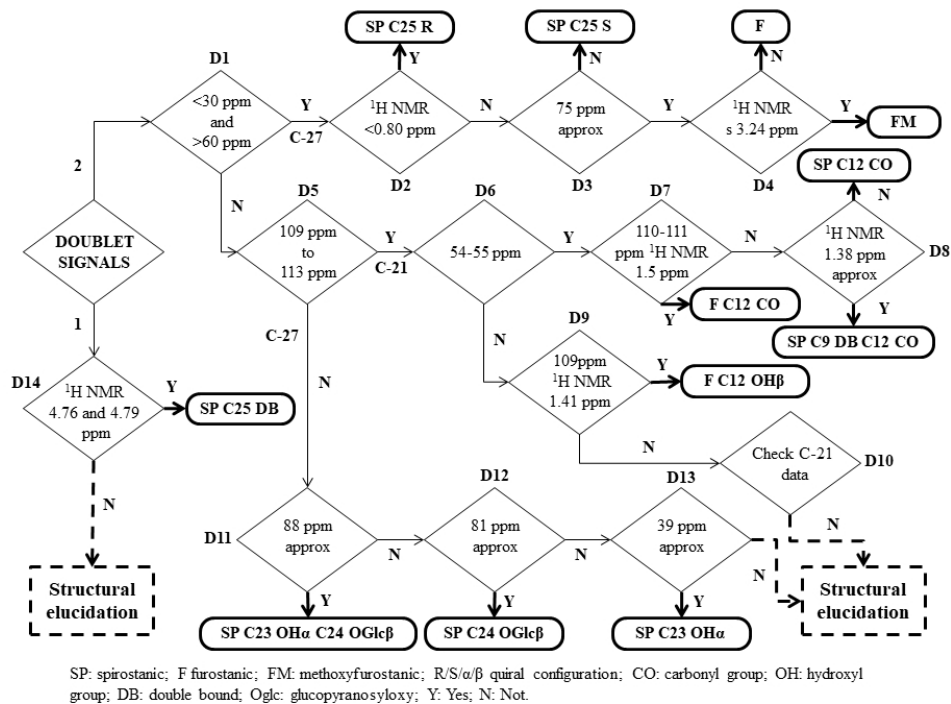


Figure 7 Flowchart for the HMBC method for aglycone identification (HMAI) of saponins from Agave species for doublet signals.

254x190mm (96 x 96 DPI)



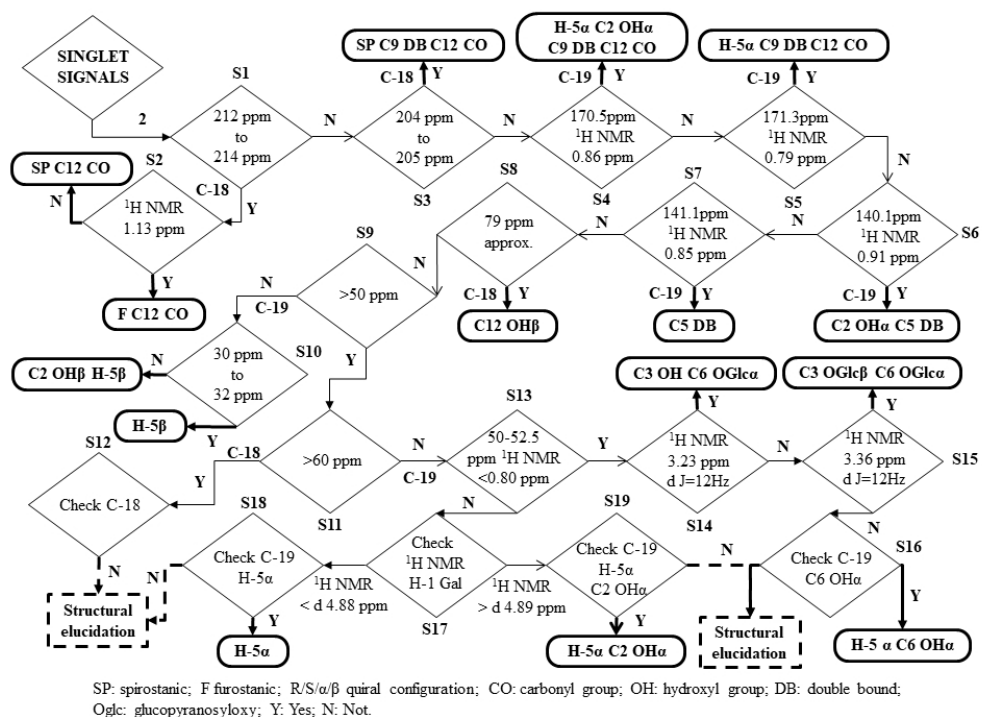


Figure 8 Flowchart for the HMBC method for aglycone identification (HMAI) of saponins from Agave species for singlet signals.

254x190mm (96 x 96 DPI)

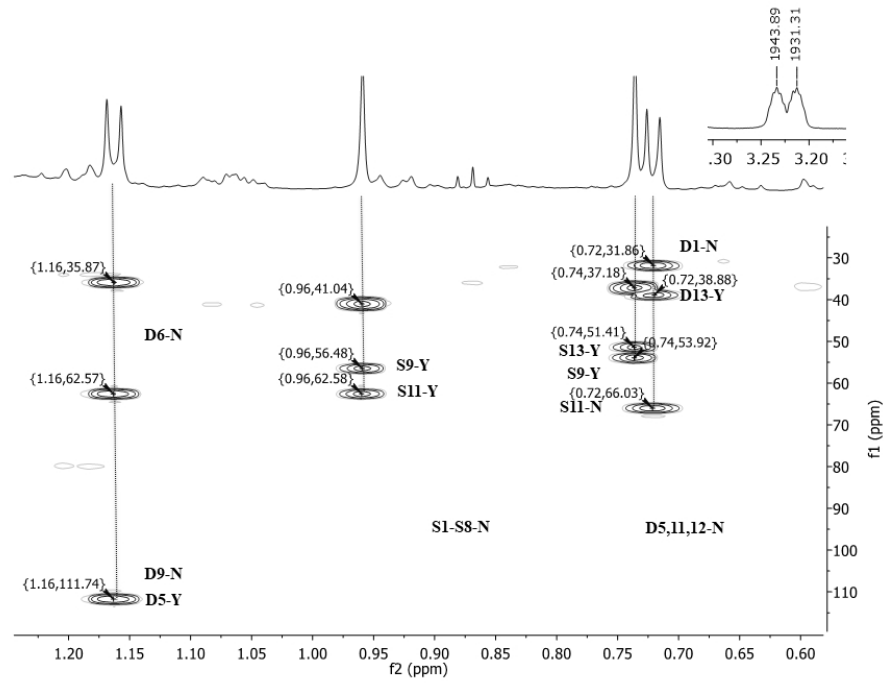


Figure 9 1H NMR and HMBC data with a representation of HMAI decisions applied.

254x190mm (96 x 96 DPI)